buildings

Article

Model Analysis of Steel Frame Structures Considering Interactions between Racks and the Frame

Weiguang Zhang, Chaoqun Yu and Genshu Tong *

College of Civil Engineering and Architecture, Zhejiang University, Hangzhou 310058, China; zwgfocus@zju.edu.cn (W.Z.); 21912047@zju.edu.cn (C.Y.)
* Correspondence: tonggs@zju.edu.cn

Abstract: The steel racks on the floor are seen as live loads in the current design process, ignoring the interaction with the supporting frames. In this paper, multiple steel racks with different masses and stiffnesses are placed on the first floor of a two-story main structure to form different real structures (RS). The corresponding simplified structures (SS) are frames with the mass of steel racks concentrated on the first floor of the main structure. Modal analysis is performed to analyze the relationship between the periods of RS and SS in the cross-aisle direction. Firstly, the beams on the first floor are assumed to be infinitely rigid. The relationship between the periods of the rack T_{Rk}, the simplified structure T_{SS}, and the real structure T_{RS} under different mass ratios α is established, and an accurate equation relating T_{RS} with T_{Rk} and T_{SS} is proposed. Moreover, by considering the influence of finite beam stiffness, the interaction between racks and the main structure is studied by constructing different analysis models. The effect of the main structure on the racks is reflected by a combined system consisting of beams and racks. A modified model, distinguished from SS by considering the effect of no-mass racks, is constructed to study the strengthening effect of the racks on the first-floor beams. The effect of the top connecting bars is also analyzed.

Keywords: rack; frame; modal analysis; period relationship; floor beam stiffness; interaction

check for updates

Citation: Zhang, W.; Yu, C.; Tong, G. Model Analysis of Steel Frame Structures Considering Interactions between Racks and the Frame. *Buildings* **2023**, *13*, 1732. https://doi.org/10.3390/buildings13071732

Academic Editor: André Rafael Dias Martins

Received: 21 June 2023
Revised: 1 July 2023
Accepted: 5 July 2023
Published: 7 July 2023

1. Introduction

In recent years, a large number of two-story warehouses have been built in China, as shown in Figure 1. The warehouse height can reach 20–25 m, and the story height is about 10–12 m. The cold-formed steel storage racks are installed on the ground and the first floor to make effective use of precious spaces.

Currently, the steel racks and main structures are designed, respectively, by rack manufacturers [1] and authorized institutes for two-story warehouses where racks are installed both on the ground and first floors. The steel racks are regarded as nonstructural components fixed to the ground [2–5]. Since the arrangement of steel racks is usually uncertain in the early design stage, the steel racks are simplified as additional live loads and the interaction between the main structures and the racks is ignored.

These two-story warehouses with racks installed on the first floor can be seen as primary-secondary combined systems, where the interaction between the primary and secondary structures can be called the Primary-Secondary Structure Interaction (PSSI), ensuring that the structure performs as a whole system. By considering the influences of PSSI, the floor response spectrum (FRS) method is applied to check the strength of non-structural members and the connections between non-structural members and supporting structures. For the calculation of primary-secondary combined systems, Sackman and Der Kiureghian [6,7] adopted the perturbation theory based on the dynamic properties of the primary and secondary structures. However, this method, based on the available literature, is only suitable when the secondary system is relatively light (usually below 1%) compared with the total mass of the whole system [8–13].

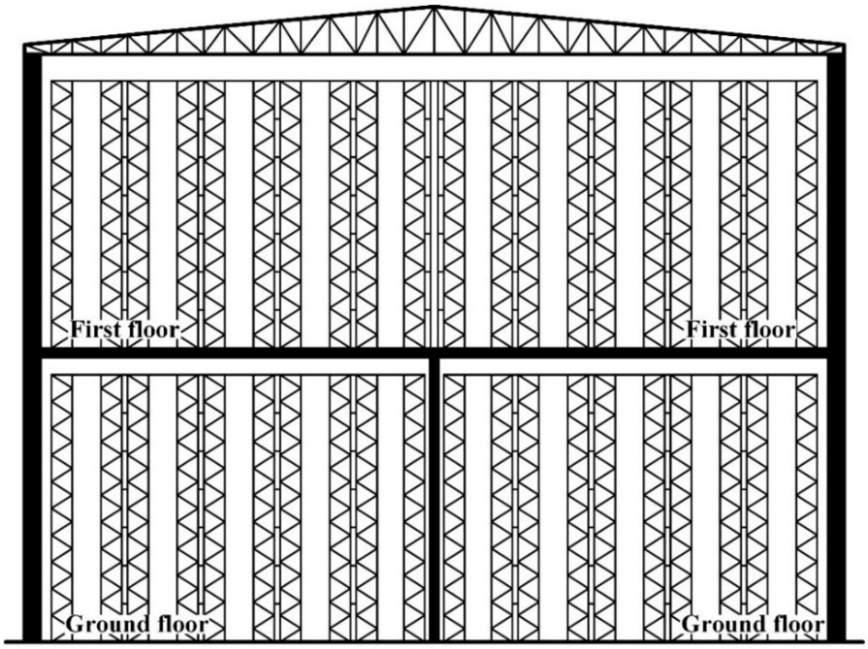

Figure 1. A Two-story Warehouse.

The FRS approach has attached much attention recently, however, these research works [14–22] concentrated on the simplified single-degree-of-freedom (SDOF) secondary system and elastic and inelastic multi-degree-of-freedom (MDOF) primary structure systems. It should be noted that secondary constructions may be connected to more than two locations in practical engineering, but the FRS method only allows for the construction of one or two points of attachment.

For the large two-story warehouse described in Figure 1, the racks on the first floor enlarge the demand on the stiffness of the floor, so the floor slabs of the main structures are generally made of reinforced concrete with thicknesses of 200–250 mm. On the first floors of the main structures, the dead load is 5–8 kN/m^2 and the live load is usually as high as 20 kN/m^2. Under these loading conditions, the mass of goods on the steel racks can account for more than 70% of the total mass of the structures. The current FRS approach is mainly for structures where the mass from the secondary equipment is very small and is not applicable for frames investigated in this paper where most of the mass is from secondary structures.

Meanwhile, the rack is a multistory structure with a height of 8 m–12 m and should be treated as an MDOF secondary system. Thus, the racks on the first floor should be considered as multiple identical MDOF secondary systems interconnected at the top. The interaction between multiple MDOF secondary systems is not considered in the current FRS approach. Therefore, a new analysis must be carried out so that the FRS approach is modified for possible future applications.

In the current design specifications involving multistory racks, no specific design requirements and methods are given for the racks installed on the first floor. It is specified in ASCE 7 [2] that when the weight of a nonstructural element is not less than 25% of the effective seismic weight of the structure, the nonstructural element is regarded as a nonbuilding structure. In addition, when the nonbuilding structure weight is not less than 25% of the combined effective seismic weights of the whole system, the different fundamental period T of the nonbuilding structure leads to different calculating methods. When T is less than 0.06 s, the nonbuilding structure should be treated as a rigid element with appropriate distribution of its effective seismic weight, and it can be simplified as an additional mass when designing the supporting structures. This method is similar to the method used when the mass of the supported nonbuilding structure is less than 25% of the mass of the combined system. However, when T is not less than 0.06 s, the supporting structure and nonbuilding structure should be regarded as a combined system with the appropriate stiffness and effective seismic weight distributions. Moreover, Chinese Codes GB50011 [23] and JGJ339 [24] only specify the seismic design method for the non-structural component of buildings when its mass is less than 10% of the floor.

A two-story frame was constructed by Zhang and Tong [25], where the racks were installed on the first floor. Dynamic history analysis on the overall structures was conducted. The elastic shear force spectra of the frames and racks were studied to verify the applicability of the simplified design method where the racks are regarded as live loads. Simplified design methods for racks and frames were proposed and the period relationship for three types of models was established. The interaction between steel racks and the main structure is considered but the influence of the floor elasticity was neglected, and the mass of racks was constant during the research, so the applicability of the period relationship needs to be further verified.

Therefore, for the two-story main structures with racks installed on the first floor, both steel racks and main structures with different first vibration periods are selected to be combined into different real structures in this paper. The following analysis will be performed in the cross-aisle (CA) direction:

(1) Modal analysis will be conducted to study the dynamic characteristics of the real structures and the simplified structures. The mass of racks is concentrated on the first floor of the main structures in the simplified structures. The relationship between the periods of the racks, the main structure, simplified structures, and real structures will be studied.
(2) The influence of the mass ratio of the rack mass to the total mass of the first floor will be involved.
(3) The influence of the floor beam stiffness will be considered.
(4) The interaction between the main structures and the racks considering the stiffness of the floor will be discussed.

The spine-bracing system is always used in the down-aisle (DA) direction to bear the weight of seismic actions [2,4], representing a different aseismic structural system. Thus, it will be examined in future studies.

2. Calculation Models and Process

2.1. Calculation Models

In this paper, a two-story structure (Figure 2d) with multiple six-story racks installed on the first floor is studied. Based on this original structure, the following four models are analyzed.

1. The first model is the steel rack. As shown in Figure 2a, the steel rack height is 9.0 m with each story possessing a height of 1.5 m. There are four rack pieces in the DA direction, and the span between rack pieces is 4.0 m. The spacing between two rack columns is 1.0 m in the CA direction, and the effective mass of each story is denoted by m. The elasticity modulus of elements in the rack is denoted by E_{Rk}, and the natural period of the steel rack in the CA direction is denoted by T_{Rk}. The value of T_{Rk} is changed by varying E_{Rk}.
2. A two-story steel frame is taken as the main structure, which is the second model and is described in Figure 2b. The spans of the main structure in two directions are both 12.0 m, and the height of each story is 10.0 m. The mass of the first floor is M_1, and the mass of the roof is M_2. The elastic modulus of the column of the main structure is denoted by E_{C}, and the elastic modulus of the beam is denoted as E_{B}. The natural period of the main structure in the CA direction is denoted by T_{SS0} (without including the masses of racks). Based on the given sections of main structural components, the period T_{SS0} will vary in the analysis through changing E_{C} and E_{B}.
3. As presented in Figure 2c, the simplified structure is the third model analyzed in this paper, which is widely used in current seismic design. The total mass of racks is concentrated on the first floor of the main structure, and the interaction between the

main structure and racks is ignored. Thus, the mass of the first floor in the simplified structure is denoted as $M_1 + n \cdot 6m$, in which n represents the number of steel racks. The natural period of the simplified structure in the CA direction is denoted by T_{SS}, which varies by changing the values of E_C and E_B. The simplified structure is abbreviated as SS in the following analysis for convenience.

4. The last model is the real structure shown in Figure 2d, which is composed of the main structure and n regularly spaced steel racks with the same stiffness. As a result, the mass of the first floor is M_1, while that of the roof is M_2. The effective mass of each story m is considered as live loads subjected to the main structure, but the active points of the live loads are at their original positions, which is different from the SS. All the racks are interconnected at their tops. The natural period of the real structure in the CA direction is denoted by T_{RS}, and the real structure is abbreviated as RS.

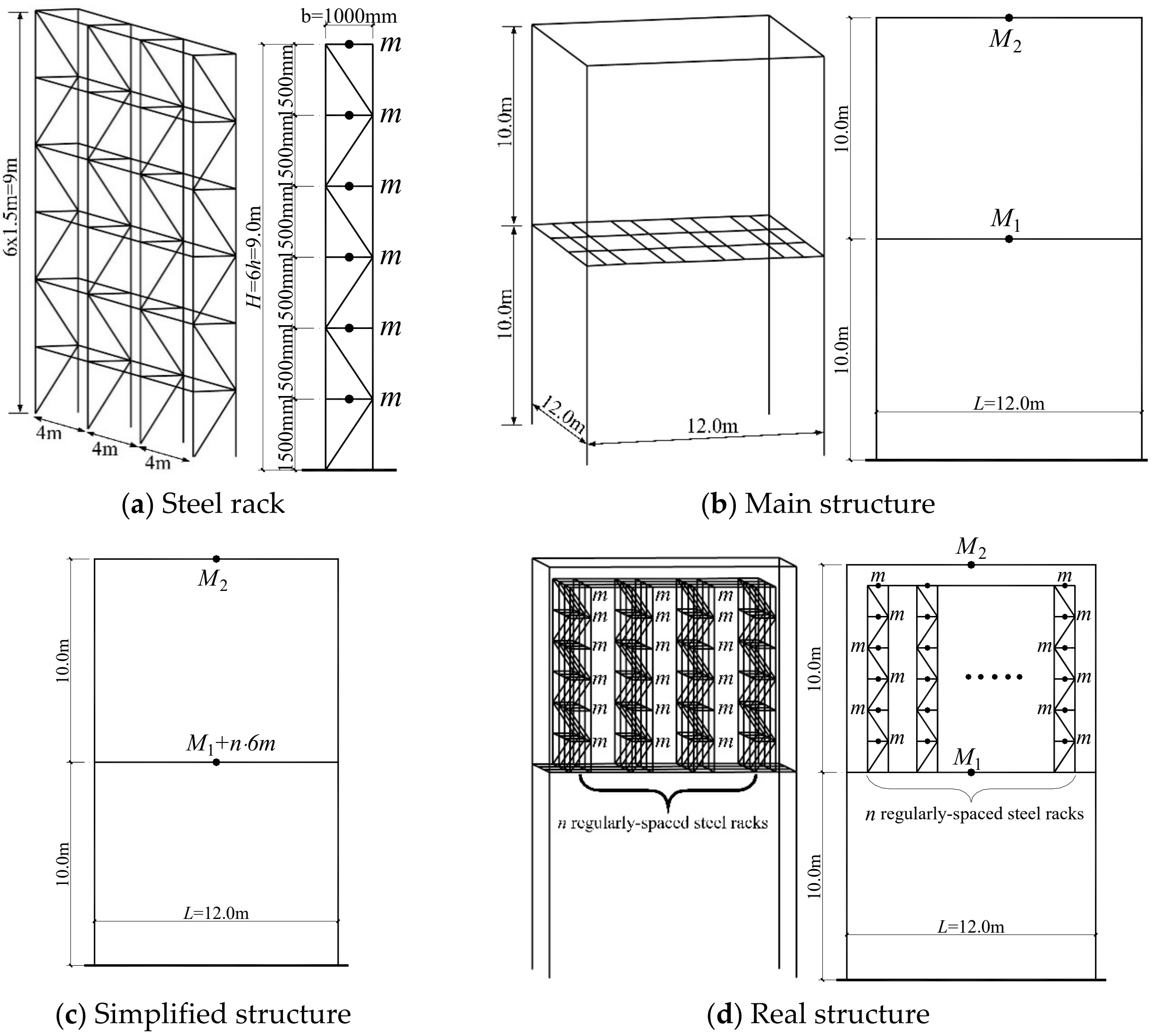

Figure 2. Analysis models.

For the convenience of calculation, the sections of calculation models stay the same during the calculation. Table 1 summarizes the details of the calculation models in OpenSees, and the initial elasticity modulus is set as $2 \times 10^6 \text{N/mm}^2$.

Table 1. The Sections of Calculation Models.

Model	Element	Section	Size (mm)			
			Depth	Flange Width	Flange Thickness	Web Thickness
Main structure	column	W14 × 211	399	401	39.6	24.9
	beam	W16 × 89	427	264	22.2	13.3
Rack	upright	W8 × 31	203	203	11	7.24
	Pallet beam	W8 × 15	206	102	8	6.22
	Upright bracing	W4 × 13	106	103	8.76	7.11

2.2. Calculation Methods and Processes

The software OpenSees [26] is used for structural modal analysis. Since a large amount of modal analysis is carried out in this paper, MATLAB is used for data analysis. The steel members of calculation models are linearly elastic since the study is intended to serve the practical design. The beams and columns are simulated by elastic beam-column elements, and the elastic truss elements are used to model the braces of the racks. For the convenience of calculation, the sections of calculation models stay the same during the calculation. In addition, the masses of the main structures in OpenSees are M_1 = 8.155 × 10^4 kg and M_2 = 2.5 × 10^4 kg. The seismic masses are assumed to be combined on the nodes in terms of numerical modeling. Furthermore, because concrete slabs are usually used on the floor, a rigid diaphragm is applied for all floors [27]. The connections between beams and columns and between columns and foundations are set to be rigid. For the real structures with racks on the first floor, the uprights of racks are simply supported on the floor beams in the models, which means that only translational restraints are given to the bottom nodes of the rack uprights.

Two types of modal analysis are firstly defined as follows:

Modal Analysis 1 (MA1): The period T_{Rk} of the steel rack remains constant, and the period T_{SS0} of the main structure changes continuously.

Modal Analysis 2 (MA2): The period T_{SS0} of the main structure remains constant, and the period T_{Rk} of the steel rack changes continuously.

The number of steel racks n and the mass of each rack story m varies during the calculation. For the convenience of calculation, the sections of calculation models stay the same during the calculation, and the change of the periods of different calculation models will be realized by changing the elastic modulus of the structural members of models.

Based on the four calculation models mentioned above, the following aspects are studied respectively:

(1) The beam stiffness of the first floor is infinite ($E_{\mathrm{B}} = \infty$), which means the influence of the elasticity of the first floor of the main structure is not considered.

Modal analysis is performed on both RSs and SSs to calculate periods T_{RS} and T_{SS}, and the relationship between T_{SS}, T_{Rk}, and T_{RS} is studied in MA1 and MA2, respectively. In these cases, the period T_{SS0} will be varied by changing the elastic modulus E_{C} of the columns of the main structure.

(2) When the beam stiffness of the first floor is finite, the relationship between T_{SS}, T_{Rk}, and T_{RS} is also studied in MA1 and MA2. In these cases, the period T_{SS0} will be varied by changing the elastic modulus E_{C} (column) and E_{B} (beam) of the main structure simultaneously.

(3) The interaction between the regularly spaced steel racks and the main structure is then studied, considering the influence of the floor elasticity of the main structure.

3. Period Relationship with Infinite Beam Stiffness

3.1. Rack Periods

As shown in Figure 2a, the period of an independent rack fixed on the ground is T_{Rk}. When this rack is installed on the first floor of the main structure (Figure 3a), the beams become the elastic support of the racks. As a result, the period of the rack installed on the first floor will change. Therefore, a combined system consisting of floor beams and racks can be constructed with the beams being fixed, and the period of this beams-racks combined system is denoted by $T'_{\mathrm{Rk}n}$, where the subscript n represents the number of racks. The combined system with one rack is shown in Figure 3b and the period is T'_{Rk1}.

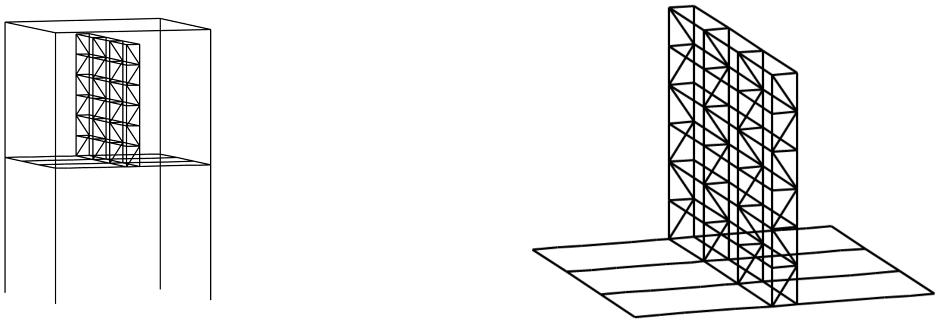

(**a**) real structure with one rack on the first floor (**b**) beams-racks combined system with one rack

Figure 3. Real structure with one rack on the first floor.

In this section, the beams of the first floor are assumed to be infinitely rigid ($E_{\mathrm{B}} = \infty$). Given the mass m of each rack floor, the elasticity modulus of the rack E_{Rk} is modified to obtain an independent rack with the period T_{Rk} = 1.0 s. The period of the beams-racks combined system with one rack can be obtained as $T'_{\mathrm{Rk1}} = T_{\mathrm{Rk}} = 1.0$ s, indicating that T_{Rk} does not change if the first-floor beams are infinitely rigid.

As the number of racks increases from 1 to 6, different beams-racks combined systems are shown in Figure 4. The connections between the racks at their tops ensure that all racks in the combined system vibrate in the same first vibration mode, as shown in Figure 5. It can be seen that without considering the influence of floor beam stiffness ($E_{\mathrm{B}} = \infty$), the number and the arrangement of racks do not affect the modal shape of beams-racks combined systems, and the periods of the six combined systems are the same, i.e., $T'_{\mathrm{Rk}n} = T_{\mathrm{Rk}} = 1.0$ s. Therefore, the vibration characteristics of the combined systems with n racks are consistent with those of the combined system with one rack whose masses and stiffness are multiplied by n (Figure 6).

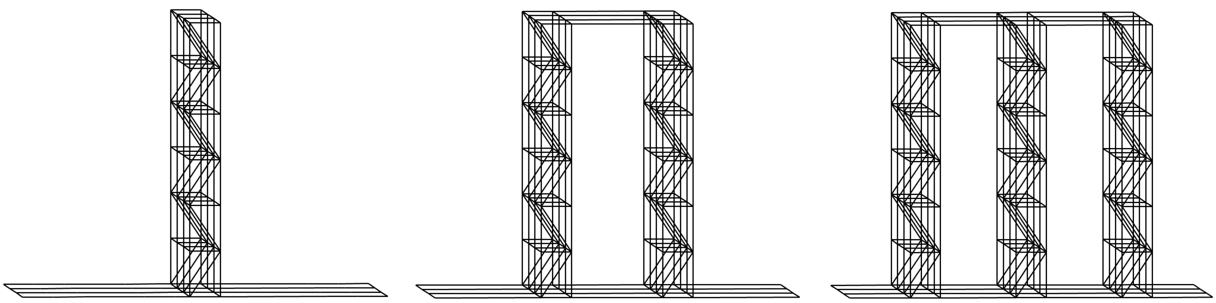

(**a**) $n = 1$ (**b**) $n = 2$ (**c**) $n = 3$

Figure 4. *Cont.*

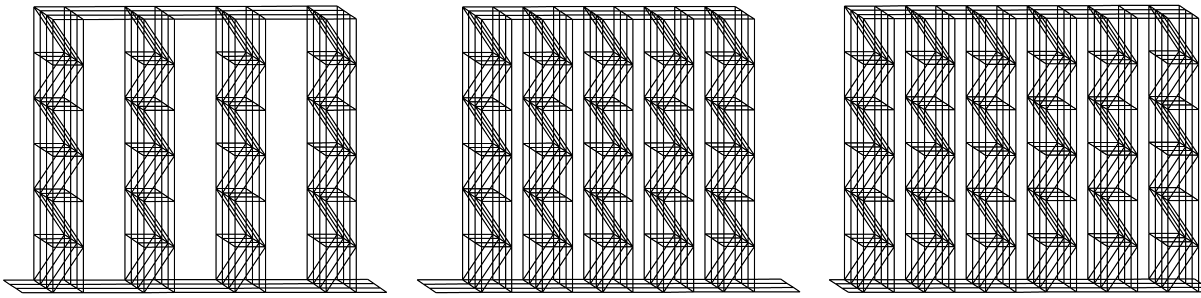

(**d**) $n = 4$ (**e**) $n = 5$ (**f**) $n = 6$

Figure 4. The beams-racks combined system with n racks.

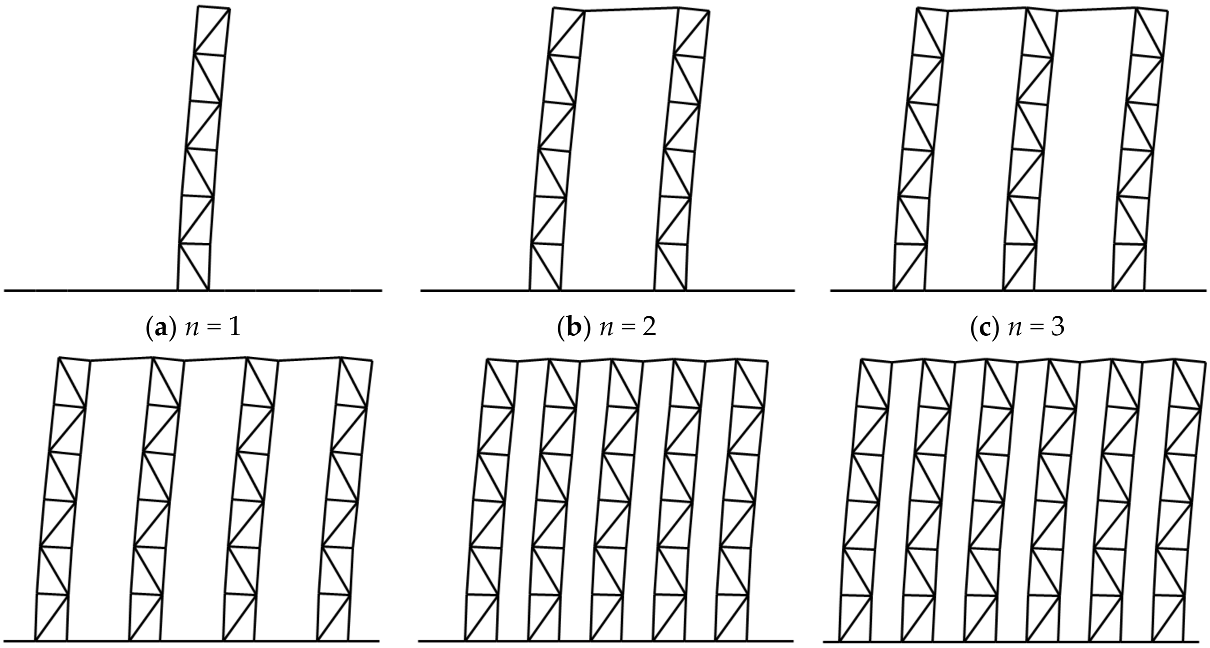

(**a**) $n = 1$ (**b**) $n = 2$ (**c**) $n = 3$

(**d**) $n = 4$ (**e**) $n = 5$ (**f**) $n = 6$

Figure 5. The first vibration modes of a beams-racks combined system with n racks ($E_B = \infty$).

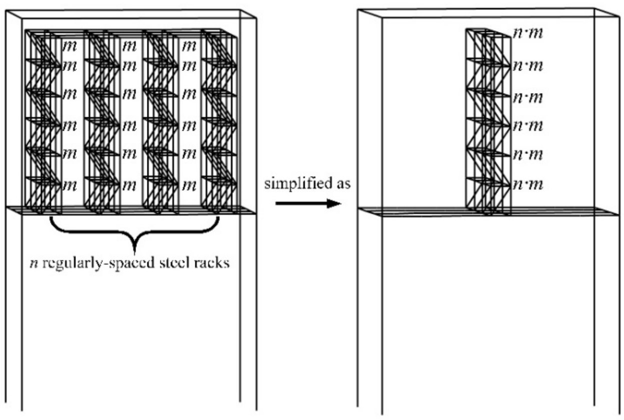

Figure 6. Simplified equivalent model in modal analysis ($E_B = \infty$).

Based on the simplified equivalent model shown in Figure 6, modal analysis will be conducted to study the relationship between the periods of the rack T_{Rk}, the simplified structure T_{SS}, and the real structure T_{RS} under two different cases:

(1) The total mass of the steel rack is constant, and the value of T_{Rk} is changed by varying the elasticity modulus E_{Rk} of the racks.
(2) The stiffness of the rack is constant, and the period T_{Rk} of the rack varies through changing the total mass of the steel rack.

3.2. Period Relationship with Constant Rack Mass

Firstly, the mass ratio α of the rack mass to the total mass of the first floor in a real structure is calculated as:

$$\alpha = \frac{6nm}{M_1 + 6nm} \tag{1}$$

The mass M_1 of the first floor of the main structure is 8.1646×10^4 kg. The mass m is firstly taken as 1.3607×10^4 kg, with which the mass ratio is $\alpha = 6nm/(M_1 + 6nm) = 0.5$, i.e., the mass of the first floor of the main structure is equal to the total mass of the racks.

Modal analysis is conducted for different real structures composed of different racks and main structures. The period T_{Rk} varies by changing the E_{Rk} of racks, and the period T_{SS0} varies by changing the elastic modulus E_C of columns. It should be emphasized that varying the period T_{SS0} will consequently change the period T_{SS} of the simplified structure in Figure 2c. Since the simplified structure is used in the current aseismic design, T_{SS} can be used directly instead of T_{SS0} in MA1 and MA2 in this section.

In MA1, T_{SS} changes continuously (0.02, 0.04, $\cdots$, 2.98, 3.0 s) while T_{Rk} remains constant (T_{Rk} = 0.1, 0.5, 1.0, 1.5, 2.0, 2.5, 3.0 s, respectively). Under this condition, modal analysis is conducted on a total of 1050 real structures. Taking the simplified structure period T_{SS} as the abscissa, seven T_{RS}–T_{SS} curves corresponding to the seven T_{Rk} are obtained in Figure 7a.

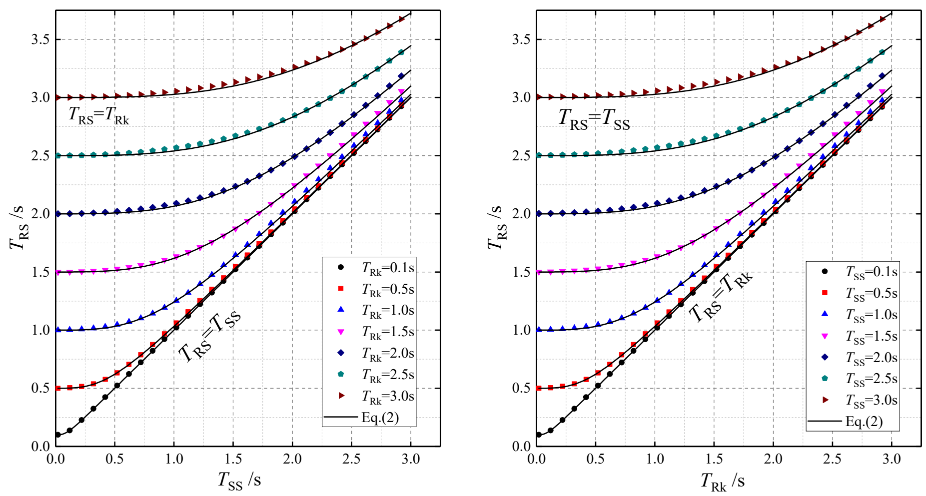

(**a**) T_{RS} in MA1 (**b**) T_{RS} in MA2

Figure 7. Period relationships between three periods with a constant rack mass ($E_B = \infty$, α = 0.5).

In MA2, T_{Rk} changes continuously (0.02, 0.04, $\cdots$, 2.98, 3.0 s) while T_{SS} remains constant (T_{SS} = 0.1, 0.5, 1.0, 1.5, 2.0, 2.5, 3.0 s, respectively). Under this condition, modal analysis is conducted on a total of 1050 real structures. Taking the period T_{Rk} as the abscissa, seven T_{RS} –T_{Rk} curves corresponding to the seven T_{SS} are obtained in Figure 7b.

From the curves in Figure 7a, it can be seen that for different T_{Rk}, each T_{RS}–T_{SS} curve starts at T_{RS} = T_{Rk} and gradually increases to the straight line of T_{RS} = T_{SS} with the increase of T_{SS}. For T_{Rk} = 0.1 s, the T_{RS} curve is basically coincident with this straight line. The curves in Figure 7b obtained in MA2 assume a similar pattern: each T_{RS} curve starts at T_{RS} = T_{SS} and gradually increases to the straight line of T_{RS} = T_{Rk} with the increase of T_{Rk}.

As the effects of T_{SS} and T_{Rk} on T_{RS} are mathematically the same, the relationship between the three periods can be accurately expressed by Equation (2), which is obtained according to the least squares method. The comparison between the numerical results and Equation (2) is also presented in Figure 7. The comparison shows that the maximum deviation is only 1.0%, so Equation (2) has excellent accuracy for both MA1 and MA2.

$$T_{RS}^{3.2} = T_{Rk}^{3.2} + T_{SS}^{3.2} \quad (2)$$

The mass ratio α is constantly equal to 0.5 in this analysis procedure, and α is not considered as a variable that may affect the relation between the three natural periods. Therefore, the role of α will be addressed through parametric studies in the rest of this section.

Firstly, the mass m is set to be $m = 5.4431 \times 10^4$ kg, giving the mass ratio $\alpha = 0.8$ and indicating that the mass of the rack is four times the mass M_1. Similarly, the modal analysis in MA1 and MA2 is conducted to calculate the T_{RS}–T_{SS} and T_{RS}–T_{Rk} curves, and the results are given in Figure 8. The curves in Figure 8 have similar shapes to those in Figure 7, but the fitting equation according to the least squares method is Equation (3), which is slightly different from Equation (2). The comparison between numerical results and Equation (3) is also given in Figure 8 and the maximum deviation is only 0.8%.

$$T_{RS}^{2.5} = T_{Rk}^{2.5} + T_{SS}^{2.5} \quad (3)$$

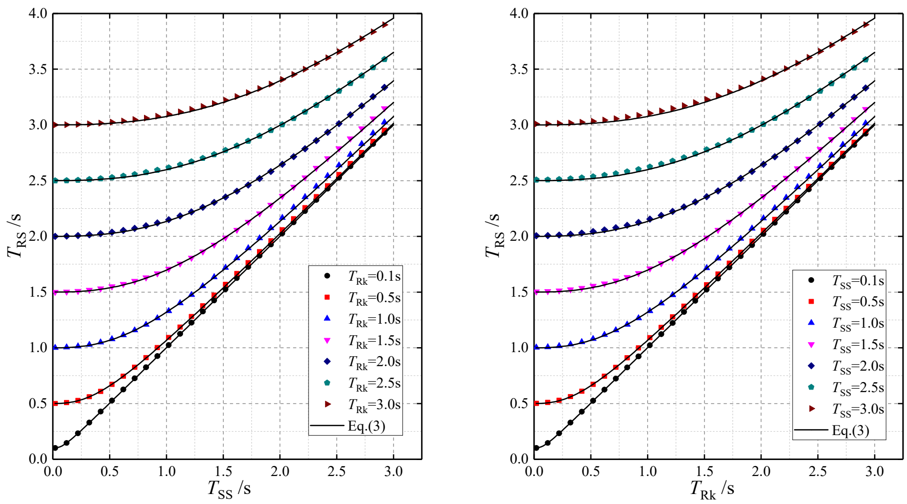

(**a**) T_{RS}–T_{SS} in MA1 (**b**) T_{RS}–T_{Rk} in MA2

Figure 8. Period relationships between three periods with a constant rack mass ($E_B = \infty$, $\alpha = 0.8$).

It can be concluded from Equations (2) and (3) that the relationship between T_{Rk}, T_{SS}, and T_{RS} for any value of α can be expressed in the form of:

$$T_{RS}^{\xi} = T_{Rk}^{\xi} + T_{SS}^{\xi} \quad (4)$$

where the power exponent ξ is dependent on the mass ratio α.

To further determine the expression of ξ as a function of α, α is set to 0.1, 0.2, 0.3, 0.4, 0.6, 0.7, and 0.9 in MA1 and MA2. Due to the symmetry of the results in MA1 and MA2, only the T_{RS}–T_{Rk} curves obtained in MA2 with different values of α are plotted in Figure 9. Meanwhile, Equation (4) is also plotted in all the subfigures of Figure 9 using the best fitting values of ξ (shown in the notation of each subfigure). The T_{RS}–T_{Rk} curves with $\alpha = 0.9$ are no longer given and the power exponent is $\xi = 2.35$. The maximum deviations between Equation (4) and the numerical results in Figure 9a–f are 0.94%, 1.07%, 1.08%, 0.92%, 0.96%, and 0.97%, respectively.

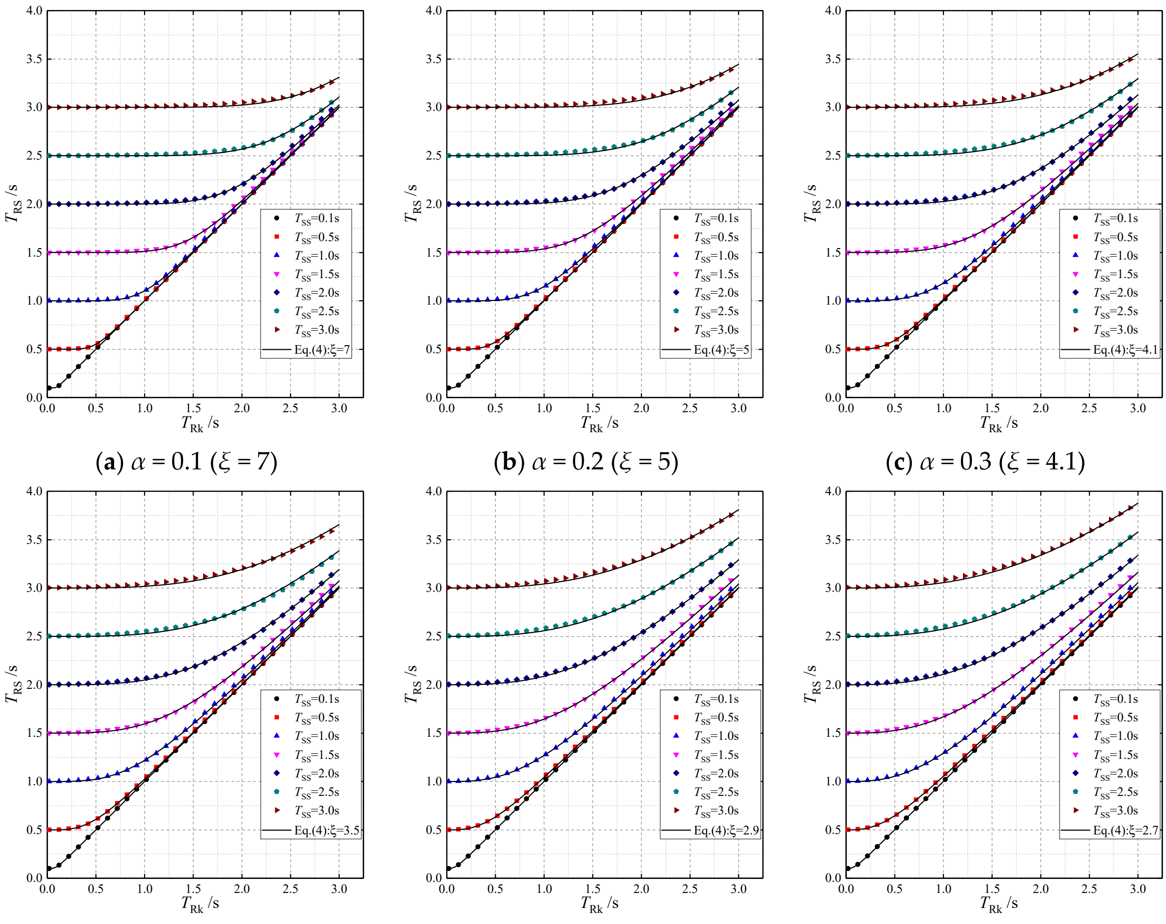

(**a**) $\alpha = 0.1$ ($\xi = 7$) (**b**) $\alpha = 0.2$ ($\xi = 5$) (**c**) $\alpha = 0.3$ ($\xi = 4.1$)

(**d**) $\alpha = 0.4$ ($\xi = 3.5$) (**e**) $\alpha = 0.6$ ($\xi = 2.9$) (**f**) $\alpha = 0.7$ ($\xi = 2.7$)

Figure 9. Period relationships with a constant rack mass ($E_B = \infty$, α = 0.1, 0.2, 0.3, 0.4, 0.6, 0.7).

According to the results shown in Figures 7–9, the relationship between the power exponent ξ and the mass ratio α is concluded as plotted in Figure 10, and the empirical expression obtained by the least squares method is proposed as Equation (5). The maximum deviation is only 1.2%.

$$\xi = \frac{2.25}{\sqrt{\alpha}} \tag{5}$$

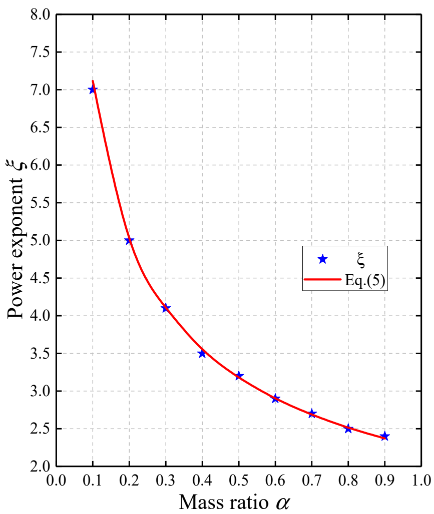

Figure 10. The relationship between the power exponent ξ and the mass ratio α.

Therefore, in the case of infinitely rigid first-floor beams ($E_B = \infty$), if the total mass of racks on the first floor of the main structure is given, the mass ratio α can be determined and subsequently the power exponent ξ is available in Equation (5). Next, the period T_{RS} of the real structure can be determined by Equation (4). Therefore, when the simplified structure is used for analysis in design practice, Equations (4) and (5) can be used to calculate T_{RS} to consider the difference between T_{RS} and T_{SS} in the simplified method.

3.3. Period Relationship with Constant Rack Stiffness

When the stiffness of the steel rack is determined (i.e., the elastic modulus E_{Rk} is constant), but the total mass of the rack is uncertain, the period T_{Rk} of the rack will vary through changing the mass of the rack. The constant elastic modulus E_{Rk} of the rack is determined following the principle that T_{Rk} = 3.0 s when the mass ratio α is 0.95. With the known E_{Rk}, T_{Rk} is 0.158 s when α = 0.05. Similarly, as T_{Rk} changes continuously (0.02, 0.04, ···, 2.98, 3.0 s), the corresponding relationship between α and T_{Rk} can be shown in Figure 11. It can be seen that the constant E_{Rk} obtained by this principle can make the mass ratio α reasonably distributed in the range of 0~0.95.

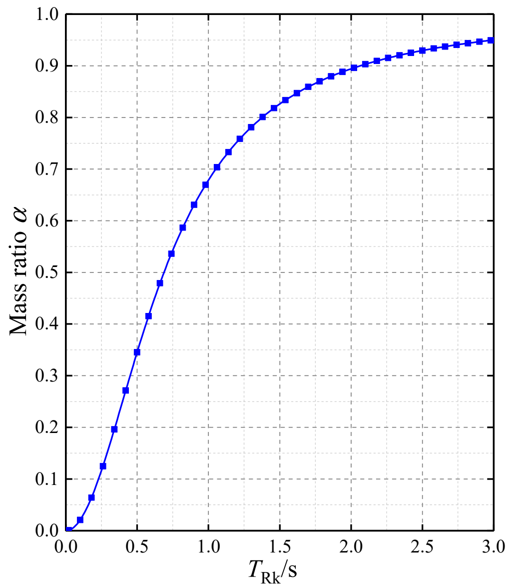

Figure 11. The relationship between T_{Rk} and the mass ratio α.

For the calculation models in Figure 2, the period T_{SS} of the simplified structure changes with the change in mass of the racks. The modal analysis is conducted on both the simplified structures and the real structures according to MA2, in which the T_{Rk} changes continuously (0.02, 0.04, ···, 2.98, 3.0 s) while T_{SS0} remains constant (T_{SS0} = 0.1, 0.5, 1.0, 1.5, 2.0, 2.5, 3.0 s, respectively). The simplified equivalent models for real structures in Figure 6 are still used in modal analysis. Therefore, T_{RS}–T_{Rk} and T_{SS}–T_{Rk} curves can be obtained corresponding to the T_{SS0} of the seven periods of the main structures, as shown in Figure 12a. Meanwhile, according to the relationship between T_{Rk} and the mass ratio α (Figure 11), T_{RS}–α and T_{SS}–α curves are shown in Figure 12b.

Since the rigidity of the rack is constant, Figure 12 shows that:

(1) For the main structure with maximum rigidity (T_{SS0} = 0.1 s), T_{RS} is basically the same as T_{Rk}, and T_{SS} hardly changes with T_{Rk} and α;
(2) For relatively flexible main structures ($T_{SS0} \geq 2.0$ s), T_{RS} is close to T_{SS} and the maximum deviation is only 6.0%, which means the simplified structure can be used in place of the real structure in modal analysis;
(3) With the decrease in T_{SS0}, (i.e., the rigidity of the main structure is gradually increased relative to the rack), the difference between T_{RS} and T_{SS} becomes more obvious;

(4) With the increase of T_{Rk}, the T_{RS}–T_{Rk} and T_{SS}–T_{Rk} curves gradually become straight lines, which means T_{RS} and T_{SS} are linearly related to T_{Rk}. Moreover, the difference between T_{RS} and T_{SS} gradually increases.

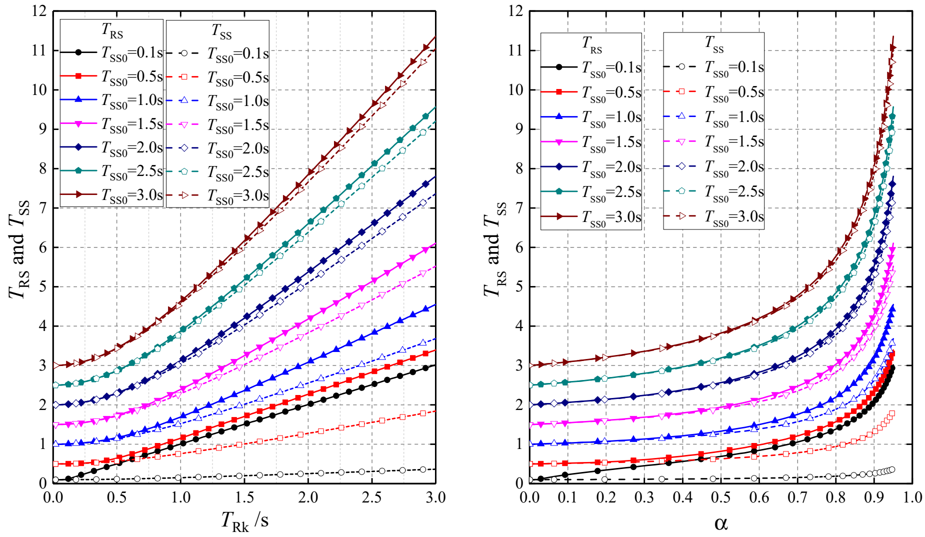

(**a**) T_{RS}–T_{Rk} and T_{SS}–T_{Rk} curves (**b**) T_{RS}–α and T_{SS}–α curves

Figure 12. T_{RS} and T_{SS} curves as a function of T_{Rk} and α with constant rack stiffness.

The numerical results of T_{RS} and T_{SS} in Figure 12 can also be used to validate Equation (4). Based on the corresponding relationship between T_{Rk} and α in Figure 11, the power exponent ξ in Equation (4) can be obtained by Equation (5), as shown in Figure 13a. Therefore, the periods T_{RS} of real structures can be calculated using Equation (4) ($T_{\mathrm{RS}}^{\xi} = T_{\mathrm{Rk}}^{\xi} + T_{\mathrm{SS}}^{\xi}$) and plotted in Figure 13b. The T_{RS}–T_{Rk} curves obtained from Equation (4) are in good agreement with the numerical results, with a maximum deviation of 0.6%.

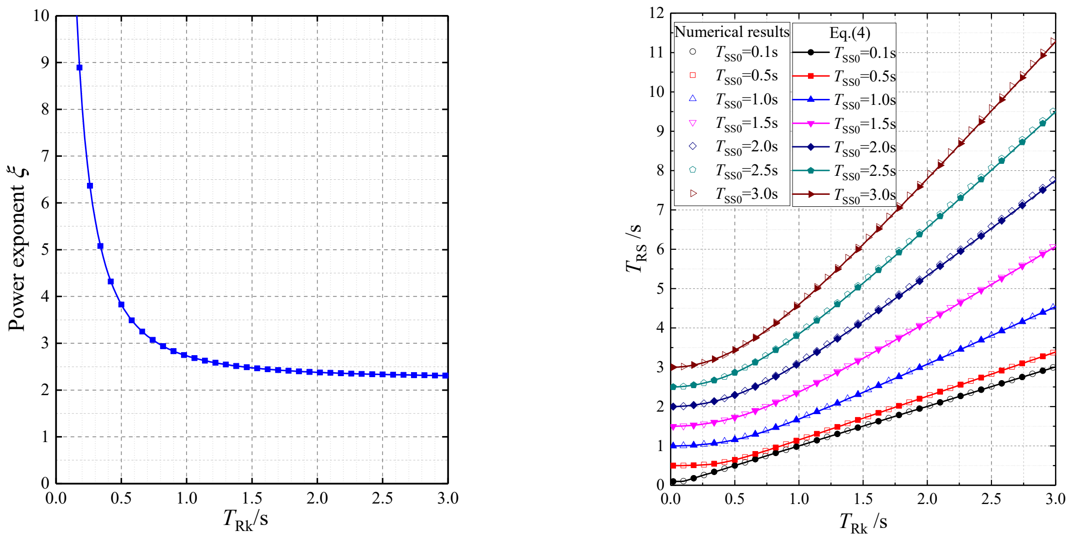

(**a**) Relationship between T_{Rk} and power exponent ξ (**b**) Numerical results and Equation (4) for T_{RS}

Figure 13. Comparison of the numerical results and Equation (4) for T_{RS} with changing rack mass ratio α ($E_{\mathrm{B}} = \infty$).

To conclude, the T_{Rk}–T_{SS}–T_{RS} relationship can be accurately expressed using Equations (4) and (5) when the influence of floor beam stiffness is not considered and the first-floor beams are assumed to be infinitely rigid ($E_{\mathrm{B}} = \infty$).

4. The Period Relationship with Finite Beam Stiffness

The T_{Rk}–T_{SS}–T_{RS} relationship, Equation (4), is based on the assumption that the first-floor beams are assumed to be infinitely rigid ($E_B = \infty$). However, the floor beam stiffness is finite in practice. Therefore, the influence of floor beam stiffness on the T_{Rk}–T_{SS}–T_{RS} relationship will be taken into account in this section.

The real structures with 1–6 steel racks installed on the first floor, as shown in Figure 14, are used in the modal analysis. For the main structure shown in Figure 2b, because the frame beam is normally heavy in such warehouses, the period T_{SS0} is mainly controlled by the elastic modulus of columns (E_C). The elastic modulus of beams (E_B) is always equal to E_C. The variation of T_{SS0} is realized by changing E_B and E_C simultaneously, and the ratio of beam-to-column stiffness i_b/i_c is constant at 0.41 according to the given sections of the main structural components in Table 1.

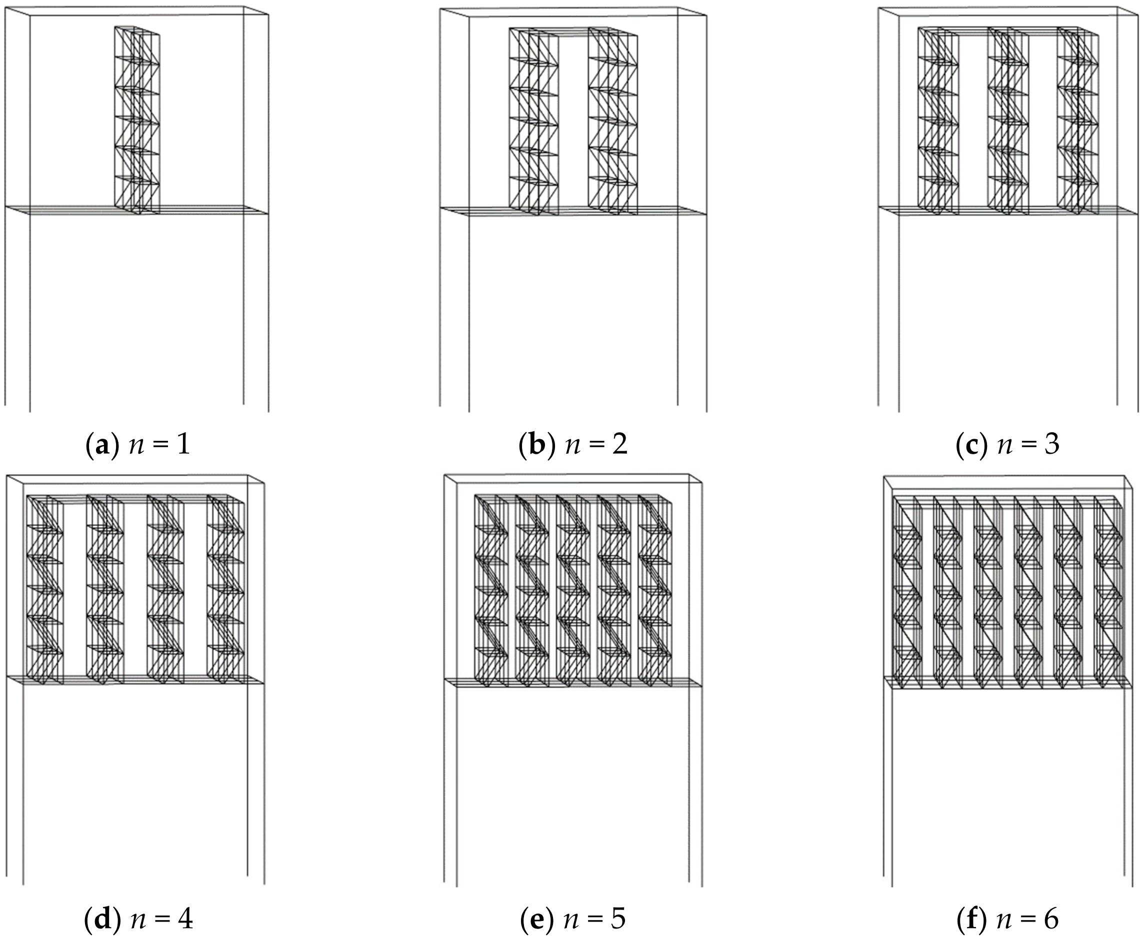

Figure 14. Real structures with n racks on the first floor.

Considering that Equation (4) is related to the mass ratio α, in order to more directly show the influence of the number of racks, the mass of racks can be prescribed as follows: The total mass of racks is prescribed (the mass ratio α is constant), and it is uniformly distributed to different numbers (n = 1, 2, 3, 4, 5, and 6) of racks on the first floor, ensuring the same period for each rack. Since the total mass of racks in engineering practices would not be very small, the mass ratio α is assumed to be in the range of 0.4–0.9.

For each constant mass ratio α, modal analysis is carried out for the six real structures in Figure 14 and simplified structures according to MA2, in which T_{Rk} changes continuously (0.02, 0.04, ⋯, 2.98, 3.0 s) while T_{SS0} remains constant (T_{SS0} = 0.1, 0.5, 1.0, 1.5, 2.0, 2.5, 3.0 s, respectively).

It should be noted that when the T_{SS0} remains constant, the changing α will consequently change the period T_{SS} of the simplified structure in Figure 2c. With different values of α, the corresponding T_{SS} values are listed in Table 2.

Table 2. Period T_{SS} of simplified structures with different values of α.

Periods of the Main Structure T_{SS0} (s)	Periods of Simplified Structures T_{SS} (s)					
	α = 0.4	α = 0.5	α = 0.6	α = 0.7	α = 0.8	α = 0.9
0.1	0.114	0.121	0.131	0.146	0.172	0.235
0.5	0.572	0.606	0.655	0.730	0.862	1.175
1.0	1.144	1.213	1.310	1.460	1.724	2.351
1.5	1.717	1.819	1.965	2.190	2.586	3.526
2.0	2.289	2.425	2.620	2.919	3.448	4.701
2.5	2.861	3.032	3.275	3.649	4.311	5.877
3.0	3.433	3.638	3.930	4.379	5.173	7.053

Firstly, modal analysis on the six real structures (Figure 14) with different T_{SS0} and T_{Rk} is conducted to obtain the corresponding T_{RS} when the mass ratio α is 0.4, as shown in Figure 15. For comparison, the T_{RS} can be calculated using Equation (4) ($T_{RS} = \left(T_{Rk}^{\xi} + T_{SS}^{\xi}\right)^{\frac{1}{\xi}}$), in which the period T_{SS} can be determined in Table 2 with the given mass ratio α and T_{SS0}. The power exponent ξ is calculated by Equation (5) ($\xi = 2.25/\sqrt{\alpha} = 3.558$). Therefore, the calculation results of Equation (4) are the same for the six real structures in Figure 14, as shown in Figure 15. It can be seen that: when T_{Rk} > 1.0 s, the maximum deviation of T_{RS} between the numerical results and Equation (4) is only 3.4%. When the racks are nearly rigid (T_{Rk} = 0.02 s) and T_{SS0} = 3.0 s, the maximum deviation is 18.9%.

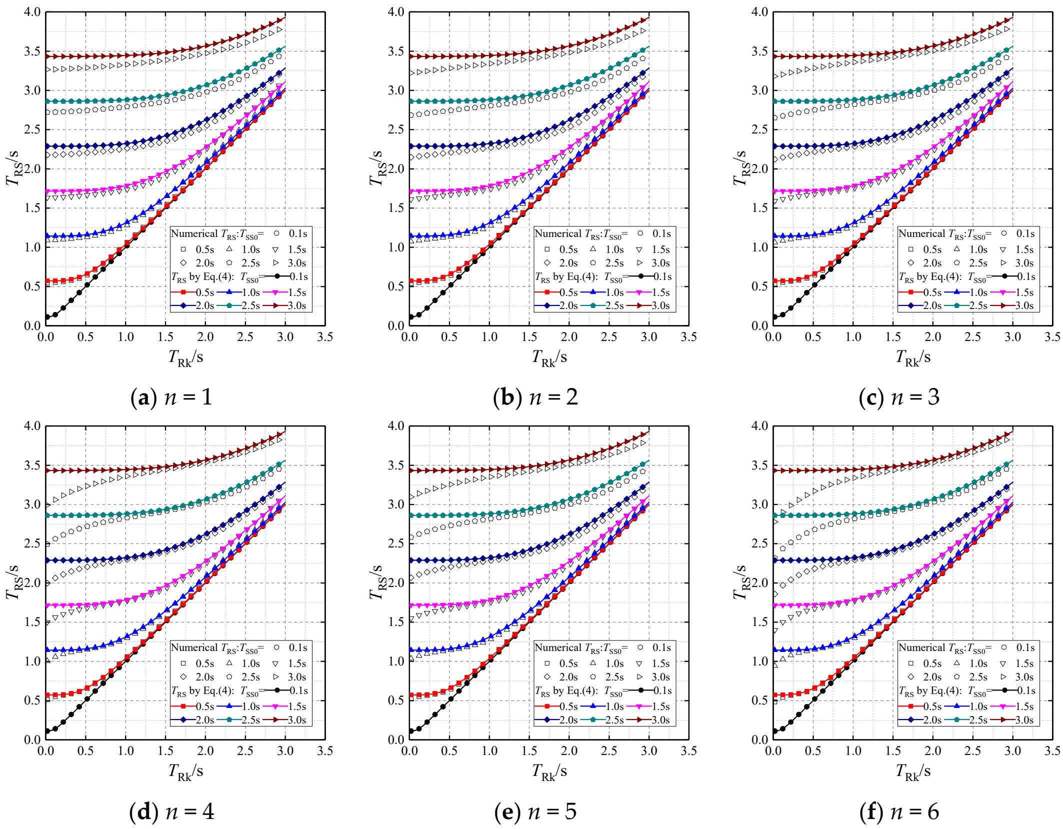

Figure 15. Numerical results and Equation (4) for T_{RS} with finite beam stiffness (α = 0.4, ξ = 3.558).

Similarly, for α = 0.6 and 0.8, the numerical results of T_{RS} are plotted in Figures 16 and 17, and T_{RS}–T_{Rk} curves obtained from Equation (4) with $\xi = 2.25/\sqrt{\alpha} = 2.905$ and $\xi = 2.25/\sqrt{\alpha} = 2.516$ are also plotted in Figures 16 and 17 for comparison, respectively. It can be seen from Figure 16 that when T_{Rk} > 1.0 s, the maximum deviation of T_{RS} between the numerical results and Equation (4) is only 4.4%. When the racks are nearly rigid and T_{SS0} = 3.0 s, the maximum deviation is 18.2%. For Figure 17, the maximum deviation is 6.6% when T_{Rk} > 1.0 s, while it increases to 17.0 when the racks are nearly rigid and T_{SS0} = 3.0 s.

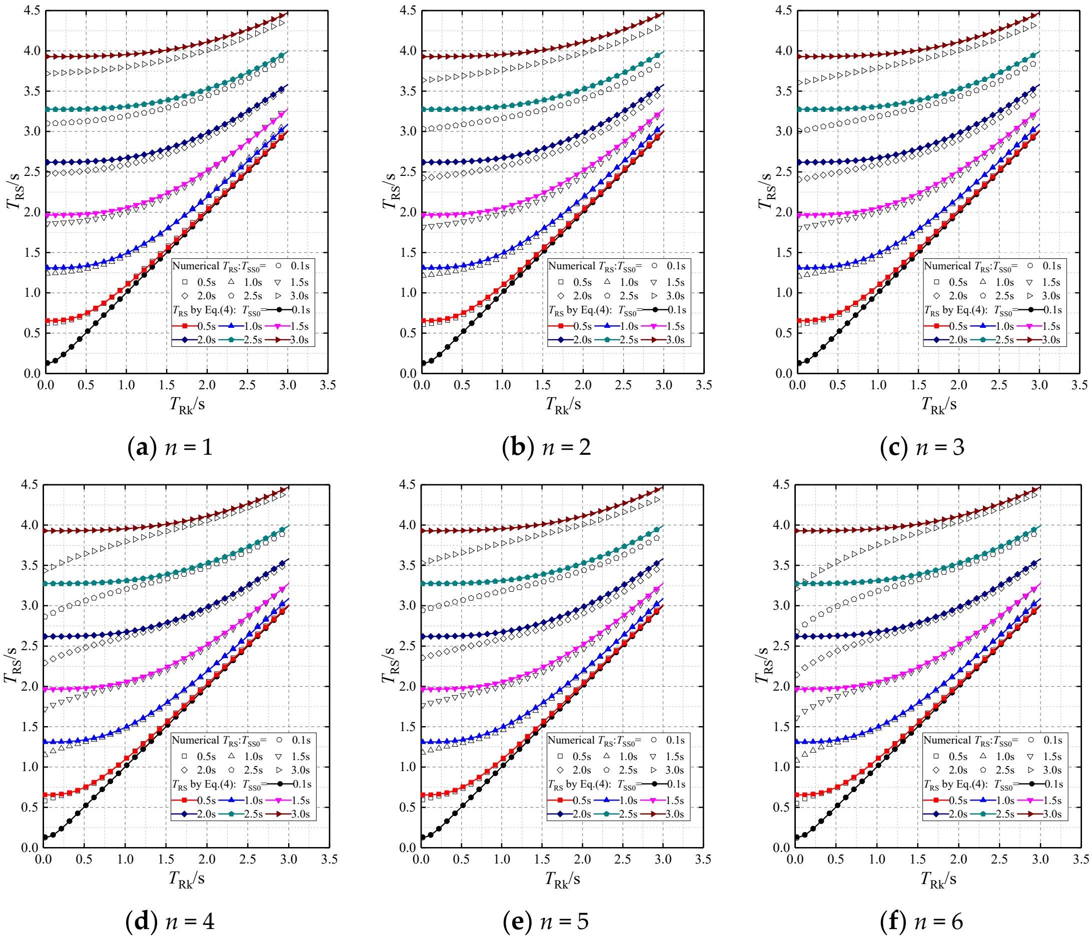

Figure 16. Numerical results and Equation (4) for T_{RS} with finite beam stiffness (α = 0.6, ξ = 2.905).

Based on Figures 15–17 illustrating the influence of finite floor beam stiffness, the following conclusions can be drawn:

(1) When T_{Rk} > 1.0 s, the numerical and theoretical (Equation (4)) results of T_{RS} are in good agreement. Therefore, Equation (4) is still applicable.

(2) When T_{Rk} < 1.0 s, the numerical results of T_{RS} are shorter than those obtained from Equation (4).

(3) With the increase of the rack number n, the difference between the numerical results and Equation (4) becomes more obvious, especially in the cases of longer T_{SS0}. Maximum differences occur when n is 6, T_{SS0} = 3.0 s, and T_{Rk} < 1.0 s, in which case the racks are relatively rigid and the floor beams are flexible.

For practical engineering, the warehouse height can reach 20–25 m, and the story height is about 10–12 m. The steel racks are essentially very tall and flexible structures, and many racks supporting heavy pallet units have periods of 1.5–2.5 s in the CA direction. When multiple racks with periods of 1.5–2.5 s are placed on the first floor of the two-story real structure, most of the mass of the real structure comes from the racks and the period of the real structure will be longer than 1.0 s. For these cases, Equations (4) and (5) proposed in this article are applicable in the design practice.

Although these differences are almost acceptable in practical engineering, the reasons for the differences should be further analyzed in the following part to include them in practice.

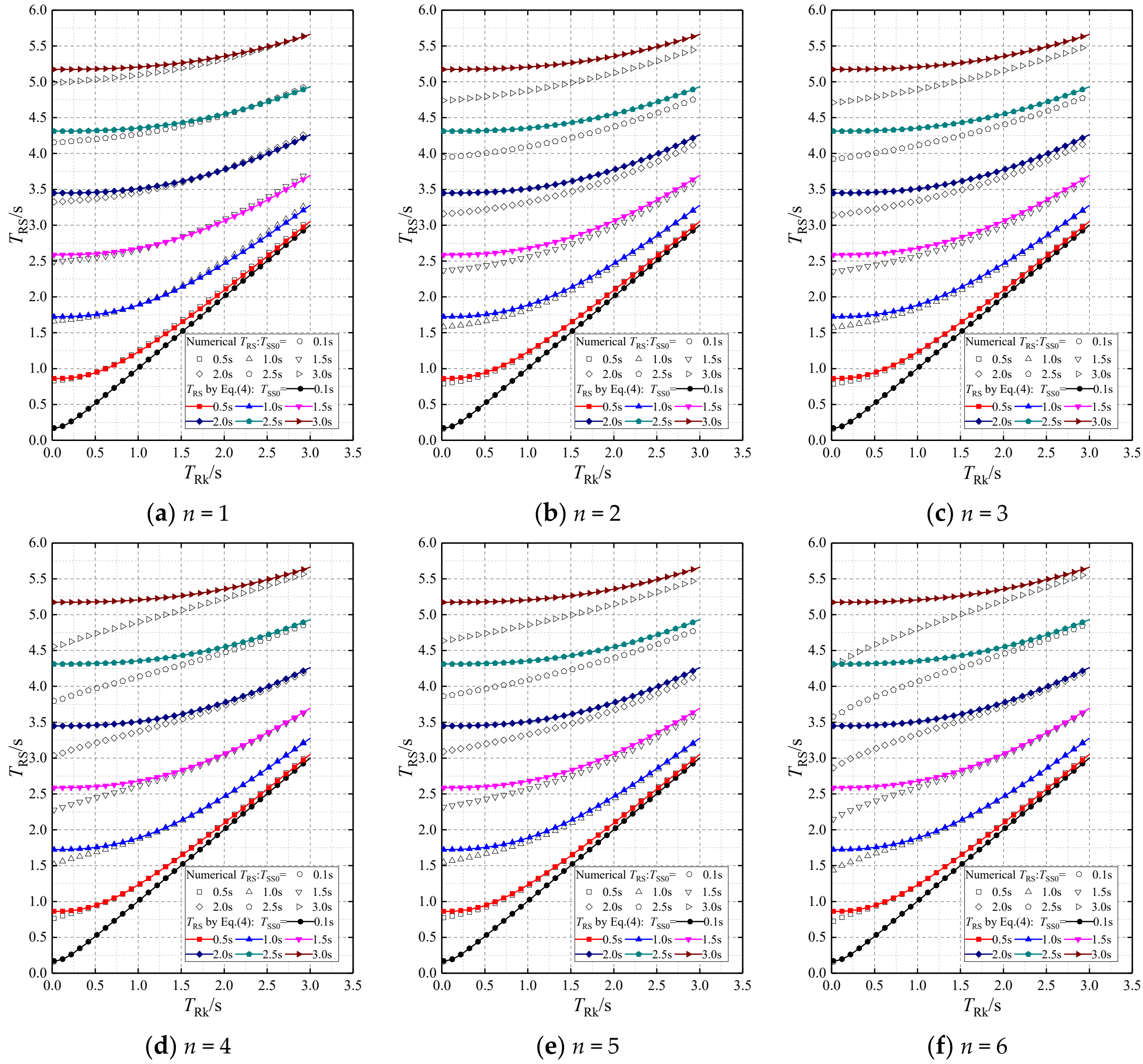

Figure 17. Numerical results and Equation (4) for T_{RS} with finite beam stiffness (α = 0.8, ξ = 2.516).

5. The Interaction between Racks and the Main Structure

Based on the above analysis, the reason for the difference between Equation (4) and the numerical results is that the interaction between racks and the main structure (mainly floor beams) has been neglected in Equation (4). In the following, the influence of the racks on the main structure and the influence of the main structure on the racks are studied by constructing different analysis models.

5.1. Influence of the Main Structure on Racks

The influence of the main structure on racks on the first floor is mainly reflected in the influence of the rigidity of the first floor beams as the elastic supports of the racks. In the case of infinite beam stiffness ($E_B = \infty$), all racks in the six combined systems (Figure 4) have the same first vibration mode in the CA direction, i.e., $T'_{Rkn} = T_{Rk}$, as seen in Figure 5

When the floor beam stiffness is finite, however, the period $T'_{\mathrm{Rk}n} \neq T_{\mathrm{Rk}}$. Therefore, the different beams-racks combined systems given in Figure 4 are selected to study the influence of the main structure on the racks. The elastic modulus E_{B} of the beams will be taken as the elastic modulus of the members when the period T_{SS0} of the main structure is 0.1, 0.5, 1.0, 1.5, 2.0, 2.5, and 3.0 s, respectively, ensuring that T_{SS0} basically covers the range of 0.02 s–3.0 s. For example, when T_{SS0} is 1.0 s, the elastic modulus of beams is denoted as E_{B} (T_{SS0} = 1.0 s).

The real structures with 1–6 steel racks installed on the first floor, as shown in Figure 14, are used in the modal analysis. For the main structure shown in Figure 2b, the period T_{SS0} is mainly controlled by the elastic modulus of columns (E_{C}). The elastic modulus of beams (E_{B}) is always equal to E_{C}, and thus, the variation of T_{SS0} is realized by changing E_{B} and E_{C}. The ratio of beam-to-column stiffness $i_{\mathrm{b}}/i_{\mathrm{c}}$ is constant at 0.41, according to the given sections of main structural components in Table 1.

Therefore, the mass ratio is set as α = 0.6 and the T_{Rk} changes continuously (0.02, 0.04, ⋯, 2.98, 3.0 s) for each elastic modulus E_{B} (T_{SS0} = 0.1, 0.5, 1.0, 1.5, 2.0, 2.5, 3.0 s). The modal analysis is conducted for the six different beams-racks combined systems to obtain corresponding $T'_{\mathrm{Rk}n}$, and the relationship between $T'_{\mathrm{Rk}n}$ and T_{Rk} is shown in Figure 18.

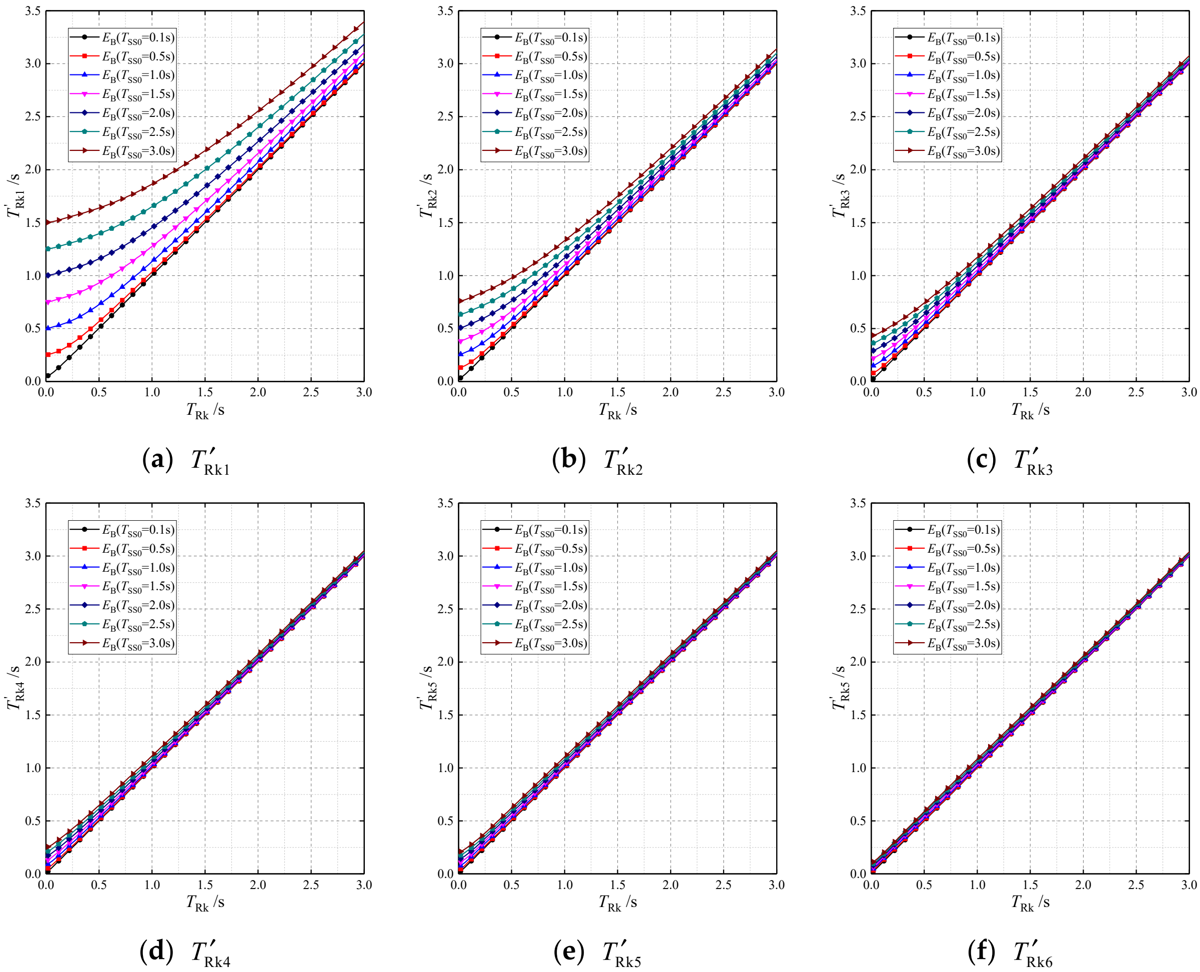

(a) T'_{Rk1} **(b)** T'_{Rk2} **(c)** T'_{Rk3}

(d) T'_{Rk4} **(e)** T'_{Rk5} **(f)** T'_{Rk6}

Figure 18. The period $T'_{\mathrm{Rk}n}$ of the six different beams-racks combined systems with finite E_{B} (α = 0.6).

It can be shown in Figure 18 that when the elastic modulus E_{B} of the beams results in a main structure period of T_{SS0} = 0.1 s, meaning that the first-floor beams are nearly rigid, $T'_{\mathrm{Rk}n}$ is closed to T_{Rk}.

For the case of the rack number n = 1, the difference between T'_{Rk1} and T_{Rk} increases gradually with the decrease in E_{B}, which means that the restraint of the beams to the racks decreases. However, as n increases, the differences become insignificant, e.g., when n = 6, Figure 18f shows that $T'_{\mathrm{Rk}n}$ and T_{Rk} are almost the same, which means the restraint to the racks is nearly rigid and the effect of beam stiffness E_{B} is small.

For the calculation of $T'_{\mathrm{Rk}n}$ of the combined system shown in Figure 19a, a simplified equivalent method (Figure 19b) can be introduced: the connecting bars between racks at their tops ensure that all racks in the combined system vibrate in the same shape, and the floor beams act as the elastic rotational restraint for the racks under horizontal vibration. The period is written out by considering the original system as the two sub-systems set up in series:

$$T'^2_{\mathrm{Rk}n} = T_0^2 + T_{\mathrm{Rk}}^2 \tag{6}$$

in which T_0 is the period when the racks are integrated as one infinitely rigid rack which is supported by a rotational spring with a stiffness of K_{Z}. Therefore, T_0 physically represents the rotational restraint of the floor beams to the racks. T_{Rk} is the period of the rack fixed on the ground.

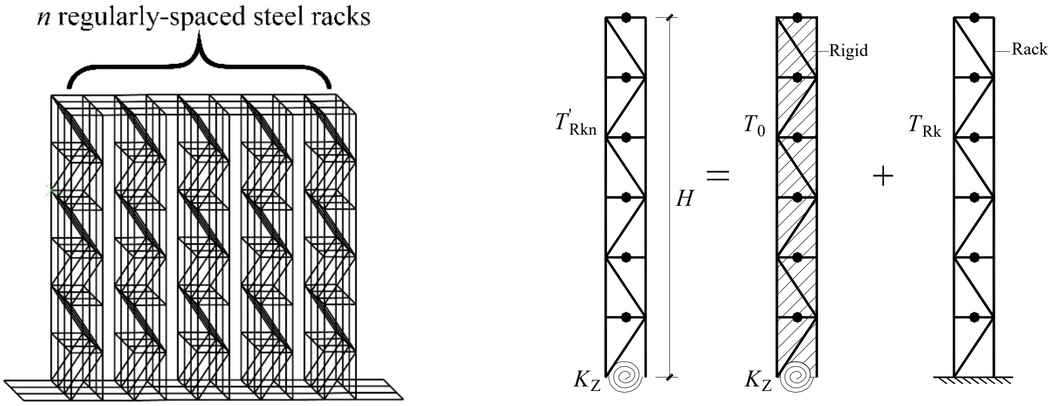

(**a**) The beams-racks combined system with n racks (**b**) The simplified equivalent model

Figure 19. The beams-racks combined systems and the simplified equivalent model.

Based on this simplified equivalent method, referring to the values of $T'_{\mathrm{Rk}n}$ in Figure 18 (α = 0.6), the period T_0 for different numbers of racks can be determined using Equation (6) ($T_0 = \sqrt{T'^2_{\mathrm{Rk}n} - T^2_{\mathrm{Rk}}}$) and plotted in Figure 20.

T_0 decreases with the increase in floor beam stiffness (E_{B}), as shown in Figure 20, and T_{RS} becomes closer to that obtained using Equation (4), which can also be concluded from Figure 16.

By comparing the curves with T_{SS0} = 3.0 s in Figure 20a–f, it is found that:

(1) In the case of n = 1, T_0 approaches the maximum value of 1.6 s, which means that the restraint of the beams to the racks is relatively minimal. The difference between T'_{Rk1} and T_{Rk} also reaches the maximum. However, as illustrated in Figure 16a, the numerical results of T_{Rk} are approximated to those obtained from Equations (4) and (5) with good accuracy.

(2) In the case of n = 6, the maximum value of T_0 is only 0.5 s and T_0 decreases further in the short period range of T_{Rk} < 1.0 s, which means the difference between T'_{Rk6} and T_{Rk} is small and the restraint of the beams to the racks is nearly rigid. However, as depicted in Figure 16a, the maximum difference of T_{RS} between the numerical results and the prediction of Equation (4) occurs exactly within this range.

Therefore, in the period range of long T_{SS0} and short T_{Rk} in Figure 16, the differences between numerical results and Equation (4) are not due to the influence of the floor beams on the racks.

Comparing Figures 18 and 20, it can be seen that such differences are basically consistent with the trend of T_0 curves. Based on the simplified equivalent method for $T'_{\mathrm{Rk}n}$

in Figure 19b, the decrease in T_0 is due to the increase in K_Z, which means the reversed rotational constraint of racks on the beams also increases gradually. Therefore, the differences of T_{RS} between numerical results and Equation (4) are probably caused by the strengthening effect of the racks on the floor beam stiffness, which will be discussed in detail in the following.

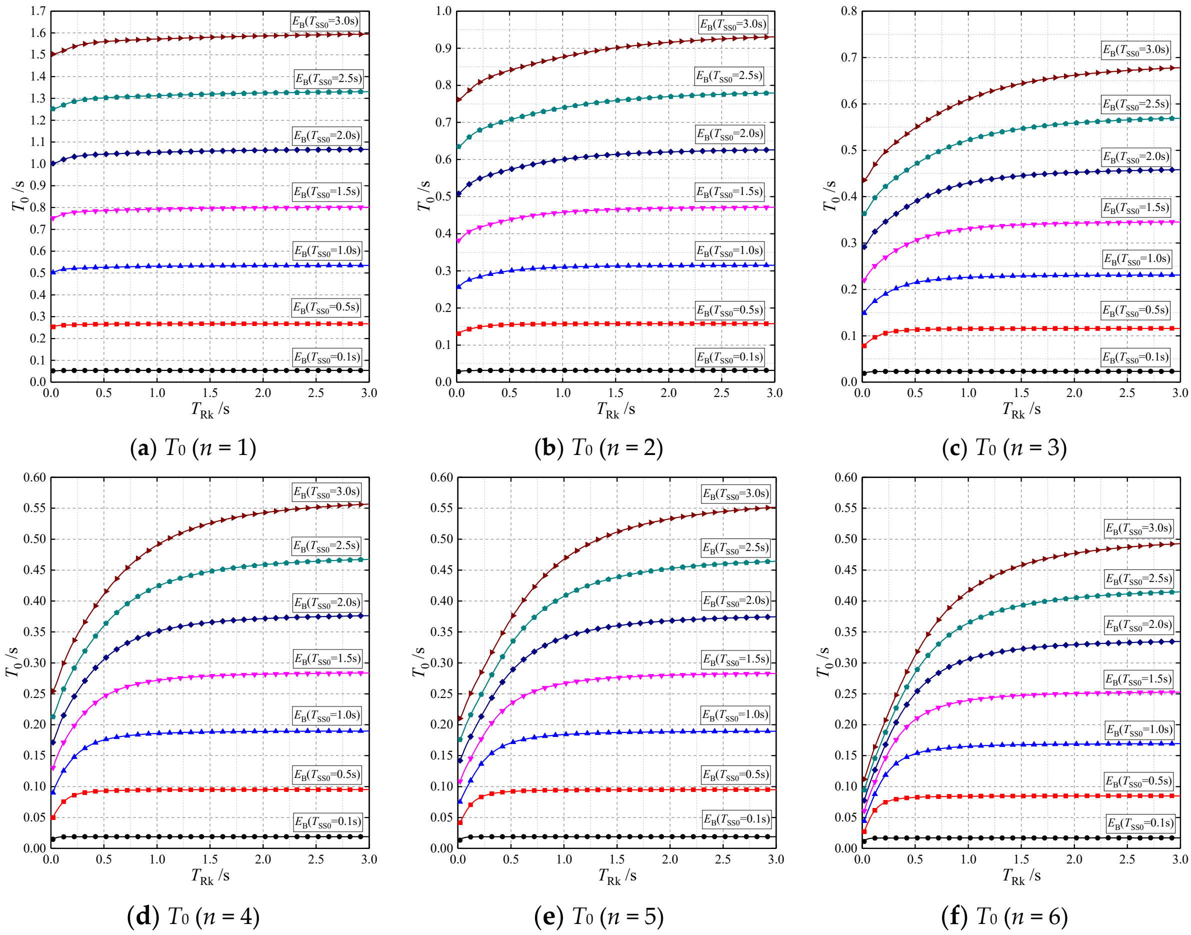

Figure 20. The period T_0 of the six different beams-racks combined systems with finite E_B (α = 0.6).

5.2. Influence of Racks on the Main Structure

The racks may increase the stiffness of the first floor, and this can be studied using the new model shown in Figure 21. This modified model reserves the racks but integrates the total mass of the racks into the first floor of the real structure. This modified model is distinguished from the simplified structure in Figure 2c by taking into account the effect of the no-mass racks, so the period of this modified model is denoted by T'_{SS}. Therefore, the analysis of the influence of the racks on the main structure can be obtained by comparing the periods of the simplified structure (T_{SS}) with the periods of the modified model (T'_{SS}).

The analysis started with the case leading to the maximum difference in T_{RS} between numerical results and Equation (4) in Figure 16, in which T_{SS0} = 3.0 s, n = 6, and α = 0.6. In this case, the period T_{SS} is 3.93 s. The T_{RS} obtained from Equation (4) ($T_{RS}^{\xi} = T_{Rk}^{\xi} + T_{SS}^{\xi}$) is larger than the numerical result, especially when T_{Rk} < 1.0 s.

For the new modified model with no-mass racks in Figure 21, the influence of the different racks is included by setting different values of E_{Rk} corresponding to T_{Rk} = 0.1, 0.5, 1.0, 1.5, 2.0, 2.5, and 3.0 s. Modal analysis on modified models with these different racks is conducted. The obtained T'_{SS} are listed in Table 3, and corresponding modal shapes are plotted in Figure 22a–f. For comparison, the modal shape of the simplified structure without racks (T_{SS} = 3.93 s) is also given in Figure 22g.

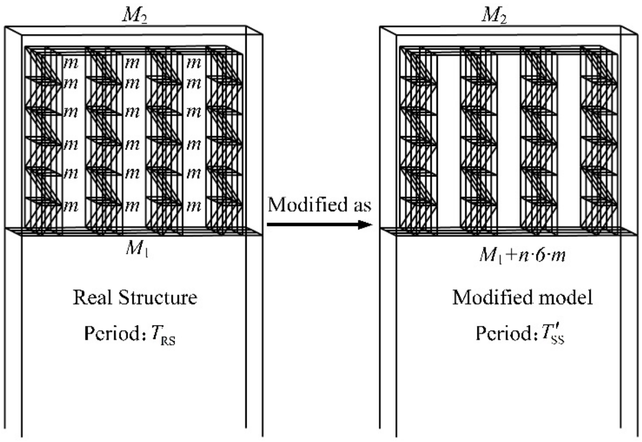

Figure 21. The new modified model based on the real structure.

Table 3. Period T'_{SS} of the modified model with no-load racks (n = 6, α = 0.6).

T_{SS0} (s)	T_{Rk} (s)	T_{SS} (s)	T'_{SS} (s)	Frame Beam Amplitude of Simplified Structure (mm)	Frame Beam Amplitude of Modified Model (mm)
3.0	0.1	3.93	3.29	6.16	0.49
	0.5		3.53		2.08
	1.0		3.70		3.77
	1.5		3.79		4.71
	2.0		3.84		5.22
	2.5		3.87		5.51
	3.0		3.88		5.69

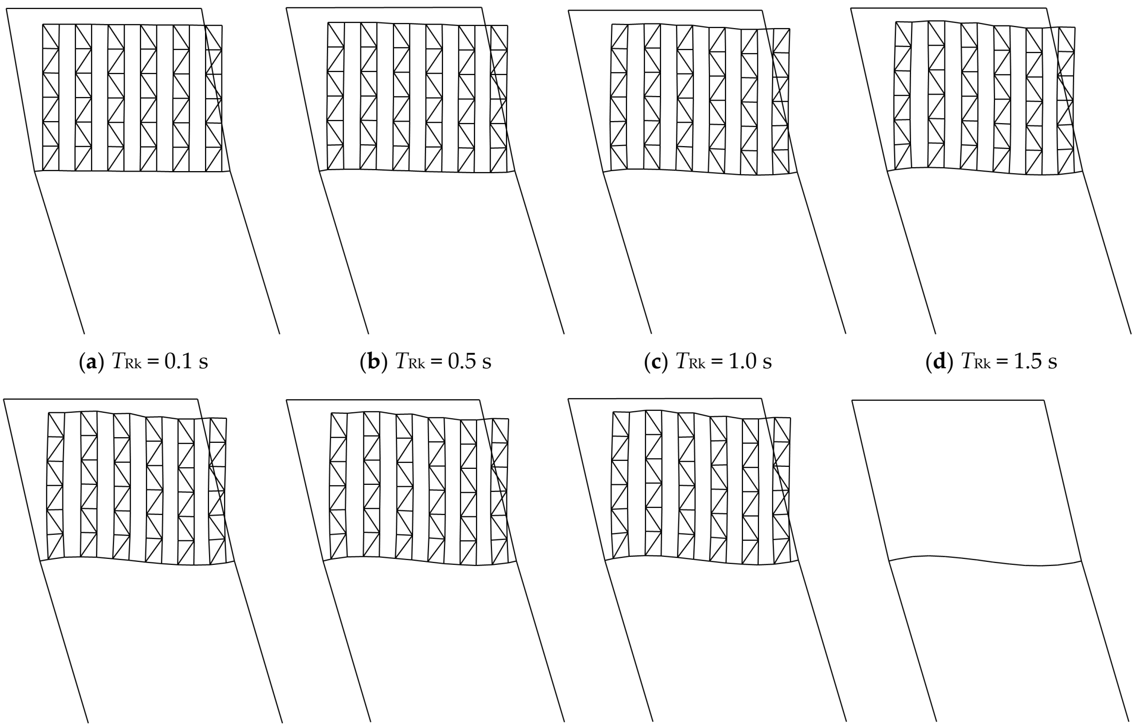

(**a**) T_{Rk} = 0.1 s (**b**) T_{Rk} = 0.5 s (**c**) T_{Rk} = 1.0 s (**d**) T_{Rk} = 1.5 s

(**e**) T_{Rk} = 2.0 s (**f**) T_{Rk} = 2.5 s (**g**) T_{Rk} = 3.0 s (**h**) T_{SS} = 3.93 s

Figure 22. The first modal shapes of modified models and simplified structures.

It is seen in Table 3 that T'_{SS} is always shorter than T_{SS} and the difference increases with the increase in the rack stiffness. Combined with Figure 22 for the first modal shape, it is found that with the increase in rack stiffness, the deflection amplitude of the floor beam in the vibrational mode becomes smaller. The specific deflection values of the first vibration amplitude are given in Table 3.

When T_{Rk} = 3.0 s, the racks have a small effect on the stiffness of the frame beam. The vibration amplitude of the frame beam is 92.3% of that in the simplified structure shown in Figure 22h with the corresponding T'_{SS} = 3.88 and s = 0.99T_{SS}. Thus, the vibration characteristics of the two models are almost identical. In this case, the value of T_{RS} obtained from numerical results is basically equal to that obtained from Equation (4), as shown in Figure 16f.

On the other hand, when T_{Rk} = 0.1 s, the frame beam of the first floor is almost rigid, and the vibration amplitude is only 8% of the amplitude in the simplified structure, and T'_{SS} = 3.29 and s = 0.837T_{SS}. Therefore, the racks with high rigidity increase the stiffness of the floor beams and contribute to reducing the period of the simplified structure. However, in Equation (4) which represents the simplified design method, this strengthening effect has not been included in the simplified structure, thus a long T_{SS} leads to a longer T_{RS} obtained from Equation (4) than the numerical results, as shown in Figure 16f.

The role of the connecting bars between racks in this strengthening effect should also be addressed in this section. Modal analysis is conducted on the modified model in Figure 21, without connecting bars between the top of racks. Similarly, given T_{SS0} = 3.0 s and different values of E_{Rk} corresponding to T_{Rk} = 0.1, 0.5, 1.0, 1.5, 2.0, 2.5, and 3.0 s, the T'_{SS} and the vibration amplitudes of frame beams are listed in Table 4. Meanwhile, the periods T_{RS} of the seven real structures in Figure 16f are also listed. The first modal shape of the six modified models without connecting bars are shown in Figure 23.

Table 4. Vibration characteristics of the modified model with/without connecting bars (n = 6, α = 0.6).

T_{SS0} (s)	T_{Rk} (s)	T_{SS} (s)	T_{RS} (s)	T'_{SS} (s)		Frame Beam Amplitude of Modified Model (mm)	
				With Bars	Without Bars	With Bars	Without Bars
3.0	0.1	3.93	3.28	3.29	3.50	0.49	3.27
	0.5		3.54	3.53	3.73	2.08	4.32
	1.0		3.75	3.70	3.80	3.77	4.92
	1.5		3.90	3.79	3.85	4.71	5.33
	2.0		4.04	3.84	3.87	5.22	5.59
	2.5		4.21	3.87	3.89	5.51	5.76
	3.0		4.41	3.88	3.90	5.69	5.86

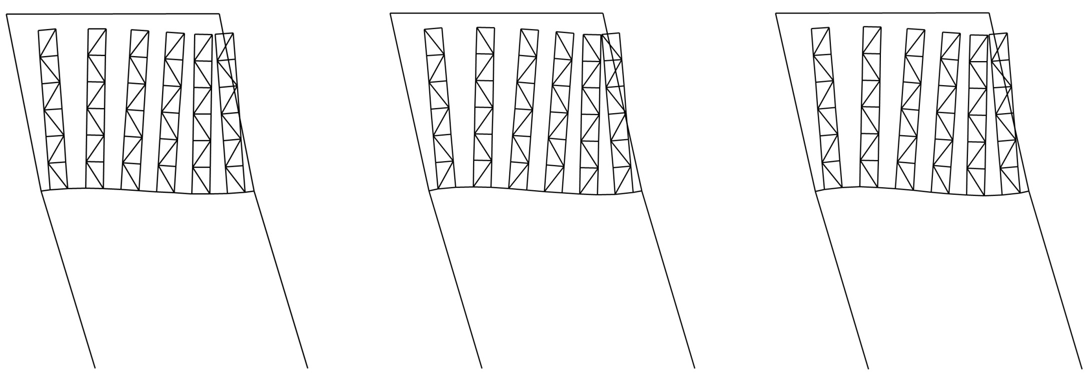

(**a**) T = 3.50 s (T_{Rk} = 0.1 s) (**b**) T = 3.73 s (T_{Rk} = 0.5 s) (**c**) T = 3.80 s (T_{Rk} = 1.0 s)

Figure 23. *Cont.*

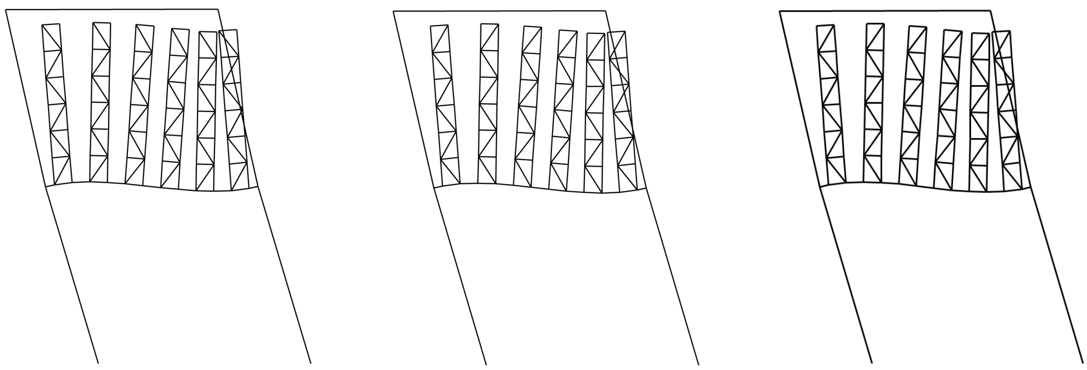

(**d**) T = 3.85 s (T_{Rk} = 1.5 s) (**e**) T = 3.87 s (T_{Rk} = 2.0 s) (**f**) T = 3.89 s (T_{Rk} = 2.5 s)

Figure 23. The first periods and modal shapes of the modified models without connecting bars.

It is found in Table 4 that, when $T_{Rk} > 1.0$ s, the T'_{SS} of the modified model with no-mass racks is not significantly affected by the top connecting bars. The modal shapes corresponding to different T'_{SS} are quite similar, as shown in Figure 23. However, when $T_{Rk} < 1.0$ s, the strengthening effect of the connecting bars on the frame beams cannot be ignored.

To further analyze the effect of connecting bars on the real structure, the real structure with T_{SS0} = 3.0 s and T_{Rk} = 0.1 s is selected, and modal analysis is conducted on real structures with and without the top connecting bars, respectively. The modal shapes of this real structure without connecting bars are plotted in Figure 24, and those of real structures with connecting bars are plotted in Figure 25.

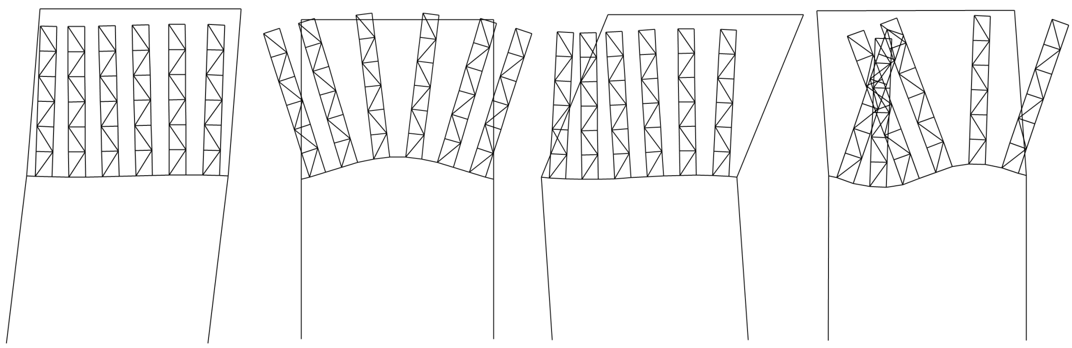

(**a**) T_{RS1} = 3.51 s (**b**) T_{RS2} = 1.35 s (**c**) T_{RS3} = 1.25 s (**d**) T_{RS4} = 0.78 s

Figure 24. The periods and modal shapes of the real structure without connecting bars.

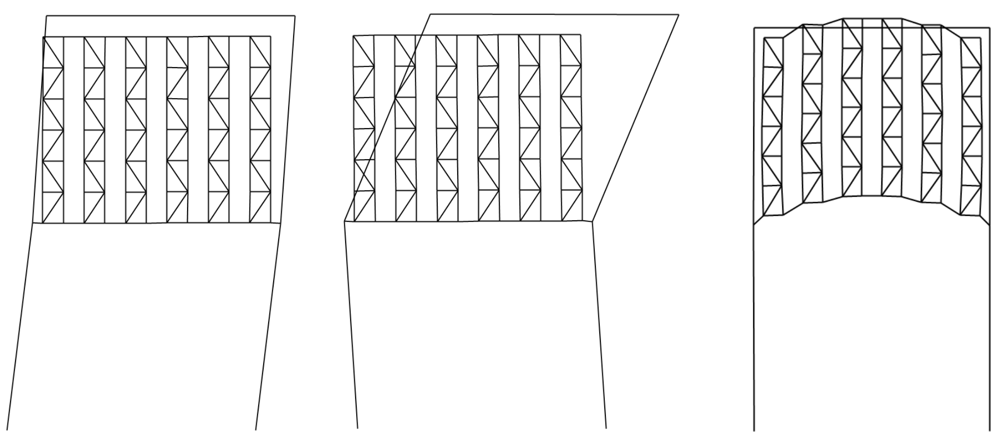

(**a**) T_{RS1} = 3.28 s (**b**) T_{RS2} = 1.22 s (**c**) T_{RS3} = 0.20 s

Figure 25. The periods and modal shapes of the real structure with connecting bars.

It can be seen that the first modal shapes are similar with or without bars, and the connecting bars reduce the first natural period of the real structure by 6.6%. The top connecting bars change the second and higher-order vibration modes.

Therefore, the strengthening effect of the racks on the beams is partly due to the high rigidity of the racks and connecting bars. The connecting bars eliminate the local vibration modes between racks and ensure that the modes of all racks are laterally consistent. As a result, the real structure will vibrate as an integrity.

Thus, Equation (4) can be modified by replacing T_{SS} with T'_{SS}:

$$T_{\mathrm{RS}}^{\xi} = T_{\mathrm{Rk}}^{\xi} + T_{\mathrm{SS}}^{\prime\xi} \tag{7}$$

in which the power exponent ξ corresponding to the mass ratio α can be obtained by Equation (5).

In order to validate Equation (7), modal analysis is conducted on the modified model shown in Figure 21 according to MA2, in which T_{Rk} changes continuously while T_{SS0} remains constant. The obtained T'_{SS} are plotted in Figure 26a, and the corresponding T_{SS} are also given. Therefore, the T_{RS} can be calculated by Equation (7) to be compared with the numerical results, as shown in Figure 26b. It can be seen that they are in good agreement and the maximum deviation is only 1.1%.

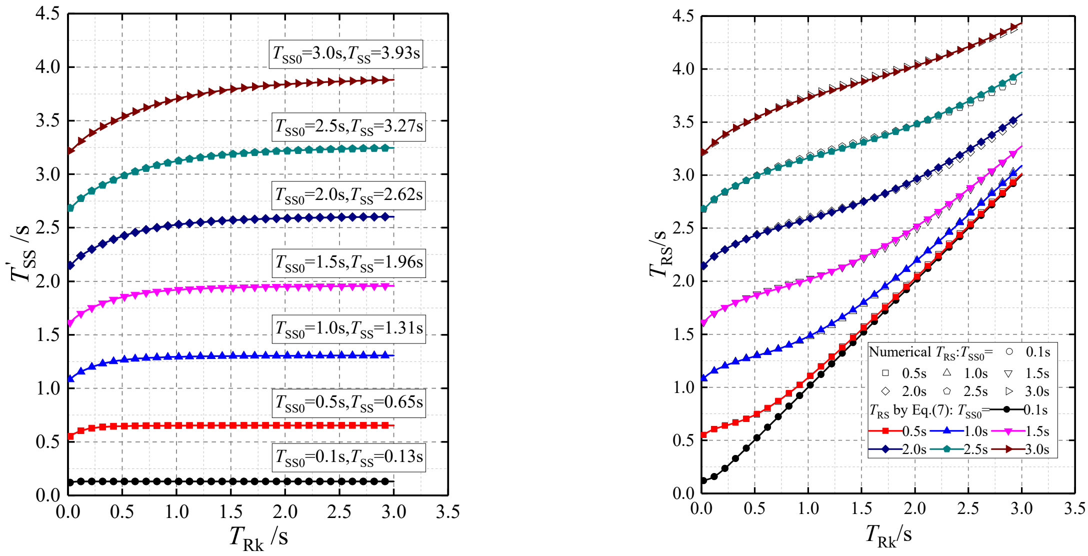

(**a**) T'_{SS} of modified model with no-mass racks (**b**) Numerical results and modified Equation (7) for T_{RS}

Figure 26. T'_{SS} of the modified model and a comparison between numerical T_{RS} and modified Equation (7) (n = 6, α = 0.6).

In addition, it is also indicated in Figure 26a that the difference between T'_{SS} and T_{SS} due to the strengthening effect of racks on floor beams is significant only in the cases where the racks are relatively rigid compared with the first floor of the main structure. With an increase in floor stiffness, the difference becomes smaller. For T_{SS0} = 3.0 s, when T_{Rk} = 0.5 s, T'_{SS} = 3.53 and s = 0.9T_{SS}, and the deviation is 10% while it was only 5% when T_{Rk} = 1.06 s. When T_{Rk} continues to increase, the influence of steel racks on the main structure floor can be neglected.

For convenience of calculation, this type of strengthening effect can be considered by multiplying the obtained period T_{RS} by a reduction factor of 0.8–0.95, similar to the effect of infilled interior walls on the period of a frame. When T_{Rk} > 1.0 s, a reduction factor of 0.95 can be used. A reduction factor of 0.8 should be used when the racks are nearly rigid and T_{SS0} is approaching 3.0 s. However, these cases rarely happen in practice, as the rigidity of the first floor is generally large as they are required to support multiple fully distributed and fully loaded racks. As the steel racks are essentially very tall and flexible structures, many racks supporting heavy pallet units have periods $T_{RK} \geq 1.5$ s in the CA direction.

Therefore, in the design practice of a real structure with racks on the first floor, the simplified structure period T_{SS} can be obtained by concentrating the mass of all racks into the first floor of the main frame. Combined with the characteristics of racks, the period T_{RS} of the real structure can be accurately predicted by Equations (4) and (5), with a suitable account of the stiffening effect of racks on beam stiffness by a period reduction factor of 0.8–0.95.

6. Summary and Conclusions

In this paper, a two-story steel frame is selected as the main structure. Steel racks with different masses, stiffnesses, and quantities are placed on the first floor of the main structure to form different real structures (RSs). The corresponding simplified structures (SS) are frames with the mass of steel racks concentrated on the first floor of the main structure. Modal analysis is performed to analyze the dynamic characteristics of RS and SS in the CA direction. The periods T_{RS} of the RSs and T_{SS} of the SSs are calculated, and the interaction between regularly spaced steel racks and the main structure is studied. The following conclusions can be drawn based on the results:

(1) When the first-floor beams are assumed to be infinitely rigid ($E_B = \infty$), the connecting bars at the top of the racks ensure that all racks vibrate in the same first vibration mode. The number and arrangement of racks have no influence on the modal shape of the real structure.

(2) When $E_B = \infty$, the relationship between the period T_{Rk}, T_{SS}, and T_{RS} can be accurately expressed by Equation (4): $T_{RS}^{\xi} = T_{Rk}^{\xi} + T_{SS}^{\xi}$, where the power exponent $\xi = 2.25/\sqrt{\alpha}$. The influence of the mass ratio α is considered, so that the relationship is applicable for the mass ratio α changing in the range of 0~1.0.

(3) The influence of the finite floor beam stiffness of the main structure on the relationship between the period T_{Rk}, T_{SS}, and T_{RS} is taken into account. When $T_{Rk} > 1.0$ s, T_{RS} predicted by Equation (4) are in good agreement with the numerical results. However, with the increase of the rack number n, the difference becomes more obvious, especially for the cases of long T_{SS0} with relatively rigid racks and flexible floor beams.

(4) With finite beam stiffness, the influence of the main structure on the racks is reflected in the influence of the rigidity of the first-floor beams as the elastic supports of the racks. Different beams-racks combined systems are selected to study the influence of the main structure on the racks. The period T'_{Rkn} of the beams-racks combined system is always greater than T_{Rk}, and the difference increases gradually with the decrease in beam stiffness, but with the increase in the number of racks (which is always the case in practice), the difference is becoming non-significant and negligible.

(5) With finite beam stiffness, the strengthening effect of the racks on the stiffness of the floor beams of the main structure is studied by constructing a new modified model, which is distinguished from the simplified structure by taking into account the effect of the no-mass racks. The racks with high rigidity and the continuous inter-connecting bars at the tops of the racks increase the stiffness of the floor beams and contribute to reducing the period of the simplified structure. The inter-connecting bars eliminate the local vibration modes between racks and ensure the modes of all racks are laterally consistent. As a result, the real structure will vibrate as an integrity.

(6) This strengthening effect leads to a shorter period T_{RS} than that predicted by Equations (4) and (5), especially in the cases where the racks are relatively rigid compared with the first floor of the main structure. This effect can be considered by multiplying the obtained period T_{RS} by a reduction factor of 0.8–0.95, similar to the effect of infilled interior walls on the period of a frame, but these cases rarely happen in practice.

Therefore, in the design practice of a real structure with racks on the first floor, the simplified structure period T_{SS} can be obtained by concentrating the mass of all racks on the first floor of the main structure. Combined with the characteristics of racks, the period T_{RS} of the real structure can be accurately predicted by Equations (4) and (5), with the mass of steel racks concentrated on the first floor of the main structure.

Author Contributions: Conceptualization, W.Z. and G.T.; Formal analysis, W.Z.; Methodology, W.Z., C.Y. and G.T.; Software, W.Z. and C.Y.; Supervision, G.T.; Validation, W.Z.; Writing—original draft, W.Z.; Writing—review & editing, C.Y. All authors have read and agreed to the published version of the manuscript.

Funding: This research received no external funding.

Data Availability Statement: The data presented in this study are available on reasonable request from the corresponding author.

Conflicts of Interest: The authors declare no potential conflict of interest with respect to the research, authorship, and/or publication of this article.

References

1. RMI (Rack Manufacturers Institute). *Specification for the Design, Testing and Utilization of Industrial Steel Storage Racks*; RMI: Charlotte, NC, USA, 2012; p. 59.
2. Federal Emergency Management Agency. *FEMA 460—Seismic Considerations for Steel Storage Racks Located in Areas Accessible to the Public*; Department of Homeland Security: Washington, DC, USA, 2005.
3. *ASCE/SEI 7-10*; Minimum Design Loads for Buildings and Other Structures, Standard. American Society of Civil Engineers (ASCE): Reston, VA, USA, 2010.
4. Castiglioni, C.A. *Seismic Behaviour of Steel Storage Pallet Racking Systems*; Springer: Cham, Switzerland, 2016.
5. *EN16681*; Steel Static Storage Systems-Adjustable Pallet Racking Systems-Principles for Seismic Design. CEN European Committee for Standardization: Brussels, Belgium, 2016.
6. Sackman, J.L.; Der Kiureghian, A.; Nour-Omid, B. Dynamic Analysis of Light Equipment in Structures: Modal Properties of the Combined System. *J. Eng. Mech.* **1983**, *109*, 73–89. [CrossRef]
7. Der Kiureghian, A.; Sackman, J.L.; Nour-Omid, B. Dynamic Analysis of Light Equipment in Structures: Response to Stochastic Input. *J. Eng. Mech.* **1983**, *109*, 90–110. [CrossRef]
8. Igusa, T.; Der Kiureghian, A. Dynamic Characterization of Two-Degree-of-Freedom Equipment-Structure Systems. *J. Eng. Mech.* **1985**, *111*, 1–19. [CrossRef]
9. Igusa, T.; Der Kiureghian, A. Dynamic response of multiply supported secondary systems. *J. Eng. Mech.* **1985**, *111*, 20–41. [CrossRef]
10. Igusa, T.; Der Kiureghian, A. Generation of Floor Response Spectra Including Oscillator-Structure Interaction. *Earthq. Eng. Struct. Dyn.* **1985**, *13*, 661–676. [CrossRef]
11. Asfura, A.; Der Kiureghian, A. Floor response spectrum method for seismic analysis of multiply supported secondary systems. *Earthq. Eng. Struct. Dyn.* **1986**, *14*, 245–265. [CrossRef]
12. Lai, M.L.; Soong, T.T. Seismic Design Considerations for Secondary Structural Systems. *J. Struct. Eng.* **1991**, *117*, 459–472. [CrossRef]
13. Qin, Q.; Nie, Y. Seismic Design and Simplified Analytical Method of Nonstructural Components and Equipment in Buildings. *J. Build. Struct.* **2001**, *22*, 15–20. (In Chinese)
14. Sullivan, T.J.; Calvi, P.M.; Nascimbene, R. Towards improved floor spectra estimates for seismic design. *Earthq. Struct.* **2013**, *4*, 109–132. [CrossRef]
15. Calvi, P.M.; Sullivan, T.J. Estimating floor spectra in multiple degree of freedom systems. *Earthq. Struct.* **2014**, *7*, 17–38. [CrossRef]
16. Calvi, P.M. Relative displacement floor spectra for seismic design of non structural elements. *J. Earthq. Eng.* **2014**, *18*, 1037–1059. [CrossRef]
17. Pozzi, M.; Der Kiureghian, A. Response Spectrum Analysis for Floor Acceleration. *Earthq. Eng. Struct. Dyn.* **2015**, *44*, 2111–2127. [CrossRef]
18. Lim, E.; Chouw, N. Review of Approaches for Analysing Secondary Structures in Earthquakes and Evaluation of Floor Response Spectrum Approach. *Int. J. Prot. Struct.* **2015**, *6*, 237–261. [CrossRef]
19. Vukobratovic, V.; Fajfar, P. A method for the direct determination of approximate floor response spectra for SDOF inelastic structures. *Earthq. Eng. Struct. Dyn.* **2016**, *45*, 2495–2511. [CrossRef]
20. Lucchini, A.; Franchin, P.; Mollaioli, F. Median floor acceleration spectra of linear structures with uncertain properties. *Earthq. Eng. Struct. Dyn.* **2017**, *46*, 2055–2060. [CrossRef]
21. Vukobratovic, V.; Fajfar, P. Code-oriented floor acceleration spectra for building structures. *Bull. Earthq. Eng.* **2017**, *15*, 3013–3026. [CrossRef]

22. Vela RJ, M.; Brunesi, E.; Nascimbene, R. Derivation of floor acceleration spectra for an industrial liquid tank supporting structure with braced frame systems. *Eng. Struct.* **2018**, *171*, 105–122. [CrossRef]
23. *GB50011-2010*; Code for Seismic Design of Buildings. China Plan Publishing Company: Beijing, China, 2016.
24. *JGJ339-2015*; Code for Seismic Design of Non-Structural Components. China Plan Publishing Company: Beijing, China, 2015.
25. Zhang, W.G.; Tong, G.S. Response spectra of two-story frames with racks on the elastic floor. *J. Build. Eng.* **2021**, *43*, 103092. [CrossRef]
26. OpenSees. *Open System for Earthquake Engineering Simulation*; Pacific Earthquake Engineering Research Center, University of California: Berkeley, CA, USA, 2021.
27. Chopra, A.K. *Dynamics of Structures: Theory and Applications to Earthquake Engineering*; Pearson Education: New York, NY, USA, 2017.